Pergamon

Int. J. Multiphase Flow Vol. 23, Suppl., pp. 1–53, 1997

Printed in Great Britain
PII: S0301-9322(97)00087-6
0301-9322/97 $17.00 + 0.00

DROPS IN ANNULAR TWO-PHASE FLOW

B. J. AZZOPARDI

School of Chemical, Environmental and Mining Engineering, University of Nottingham, University Park, Nottingham NG7 2RD, U.K.

(Received 24 October 1996; in revised form 21 November 1997)

Abstract—Drops, one of the forms in which liquid is present in annular gas–liquid flow, are formed from the wall film, carried by the gas or vapour and redeposited. During this time they exert a strong influence on many important parameters of both flow and heat transfer. The available information on the creation, size and velocity, and removal of drops is identified and reviewed.

This review shows that there is an extensive literature on drops and the associated topic of waves in annular gas–liquid flows. In spite of the large number of papers that have been published, there are still some fundamental questions which remain unanswered and there are large gaps in the parameter ranges to be considered. © 1998 Elsevier Science Ltd. All rights reserved

1. INTRODUCTION

The term annular flow is used to describe the configuration of gas–liquid flow in which some of the liquid travels as a film on the channel walls and the rest is carried as drops by the gas in the centre of the channel. The fraction of liquid travelling as drops varies from zero to close to one. Such flows, which are also termed annular-dispersed or mist flow, can occur at all pipe orientations. In vertical flow the film is uniform about the pipe circumference, but for inclined and horizontal pipes, gravity causes a significant asymmetry of the film, much higher flow rates and film thicknesses are found at the bottom than at the top of the pipe. For vertically downwards flows there are wide ranges of conditions where the liquid flows entirely as a film.

Annular flow is important because it occurs in a wide range of industrial equipment. It can be the predominant flow pattern where the quality (vapour mass fraction) is changing, such as in a boiler tube. This is best illustrated by a flow pattern map such as that of Mayinger and Zetzmann (1976) (figure 1). The abscissa can be taken as proportional to the quality which increases along the tube. Inspection of the figure shows that a significant part of the boiler tube will be in annular flow, particularly at high mass fluxes. Under such circumstances, the film flow is depleted by evaporation. In addition, it will be depleted further by the creation of drops by the vapour shear, a process that will increase as the vapour quality and thence vapour velocity and shear increase along the channel. Careful measurements by Bennett *et al.* (1969) show that as the input heat power is increased the film flow rate tends towards zero (figure 2). The condition of zero film flow rate has long been known as dryout and is particularly important because the heat transfer deteriorates significantly beyond this point. In heat flux controlled cases such as nuclear reactors this can lead to large excursions of the wall temperature and thence damage to equipment. In the fired heaters used in oil refining, the temperature excursion can result in excessive fouling (coking).

The split of liquid between wall film and drops is also important for any modelling of pressure drop. Most published methods for pressure drop have but a single description which is applied to such diverse flow patterns as bubbly, slug and annular flow. However, the latest developments are using flow pattern identifiers together with flow pattern specific models (Holt and Azzopardi 1995). For annular flow, the wall film acts as a rough wall, the extent of the roughness affecting the frictional component of the pressure drop. The roughness will depend on the flow rate of liquid in the film. In addition, there are contributions to pressure drop from the acceleration of drops from their initial, low velocity (that of the film) towards that of the gas and from the momentum transformed when drops deposit. Fore and Dukler (1995b) have

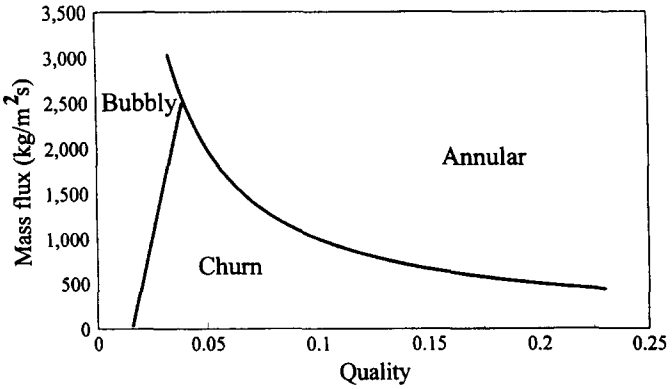

Figure 1. Flow pattern map for vertical upflow.

determined that this latter contribution increases with gas velocity and that up to velocities of 37 m/s it can reach 20% of the total pressure drop.

Drops are important in their own right, for example in considering the problem of erosion or erosion/corrosion. Here the damage done will depend on the size and velocity of the drops.

This review considers the available information about drops in annular flow under three headings: their creation (atomization or entrainment), their existence (size and motion) and their removal (redeposition on to the wall film). The review considers all orientations from vertical upflow through to vertical downflow. However, it is noted that the majority of the information is for vertical upflow. For horizontal flow, stratified as well as annular flow will be considered, where relevant.

2. CREATION— ENTRAINMENT FROM THE WALL FILM

In annular flow, the majority of drops are created from the wall film by the action of the gas flowing over it. This can be illustrated by the simple experiment in which liquid is carefully introduced as a film on the tube walls. Measurement of the film flow rate at points downstream yields monotonically lower values than at inlet.

The surface of the film is not smooth but covered with small-wavelength waves (usually termed ripples). In addition, for a wide range of conditions, there are longer-wavelength, larger-amplitude waves (usually termed disturbance or roll waves). These waves have a height several

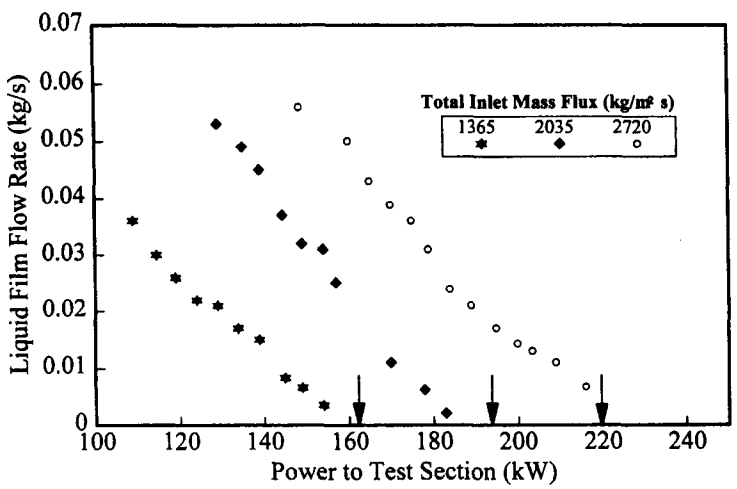

Figure 2. Variation of film flow rate with input power. (Reproduced from UKAEA Report AERE R-5809, Bennett *et al.*, "Measurement of liquid film flow rate at 1000 psi in upwards steam water flow in a vertically heated tube", Copyright (1969), with kind permission of AEA Technology plc., Harwell, UK.)

times the mean film thickness and travel at a velocity greater than that of the film. A close examination of the process of drop creation indicates that drops are not created from the entire film interface, but very specifically they arise from these disturbance waves (Arnold and Hewitt 1967; Cousins and Hewitt 1968; and Woodmansee and Hanratty 1969). The most conclusive proof that waves are the source of drops was provided by Azzopardi and Whalley (1980). They noticed that, if the film flow rate was set at a flow rate just below that required for disturbance wave creation and a small volume of liquid was suddenly injected into the film, a small number of waves are created. The flow at the top of the pipe was observed by means of a high speed cine camera used in conjunction with a special axial viewing device. Before the waves were created no drops were present. Subsequent to injection, drops were seen; the number of drops increased as the waves approached the end of the pipe. Once the waves had passed out of the pipe, no drops were seen. An additional type of wave has been identified by Sekoguchi and Takeishi (1989), These they termed huge waves. They were characterized by larger amplitudes, wavelengths and velocities than disturbance waves.

This section considers the conditions for the occurrence of disturbance waves and of entrainment, the properties of disturbance waves, methods for measurement of the rate of entrainment and equations to predict entrainment rate. It concentrates on annular flow, with occasional references to the neighbouring flow patterns of wispy-annular and churn flow (for vertical upflow) and stratified flow (for inclined and horizontal flows).

2.1. *Occurrence of disturbance waves and entrainment*

It is relatively easy to observe disturbance waves if the test section is transparent. For small diameter tubes they are visible as milky bands which are coherent about the entire periphery travelling rapidly up the tube. They are also obvious on time-traces of film thickness. In spite of their importance, the amount of theoretical work on waves in annular flow has been more limited than the experimental side. Waves on freely falling films have had much more attention. The majority of the theoretical studies have been carried out using linear stability analyses, e.g. Andreussi *et al.* (1985). A non-linear analysis has been presented by Jurman *et al.* (1989). Recently, Pols *et al.* (1996) have presented a study following the ideas of Dressler (1949) for roll waves in inclined open channels. Their study differed from Dressler in that they allowed for an interfacial shear which was of the same order as the wall shear stress; Dressler considered a flow driven by gravity with the wall shear stress much greater than that at the interface. The results gave good prediction of the wave velocity and height as measured by Miya *et al.* (1971) for stratified flows in a rectangular channel. The approach is currently being extended to vertical upflow.

The combinations of gas and liquid flow rates at which disturbance waves first appear have been recorded by a number of workers who noted that they do not occur for some flow conditions, particularly at low liquid flow rates. The pipe diameters and physical properties pertinent to individual data sets are given in table 1. In all cases the critical liquid flow rate increased with increasing gas flow rate. However, distinct effects of tube diameter, liquid viscosity and surface tension are seen in the data, even when they are plotted in terms of the respective Reynolds numbers for the phases. Azzopardi *et al.* (1983) employed dimensional analysis and suggested that the appropriate dimensionless groups to correlate this data were a liquid Reynolds number ($Re_l = \dot{m}_l D_t/\eta_l$), the Onhenzoge number ($On = \eta_l/\sqrt{(\sigma \rho_l D_t)}$) and a dimensionless gas velocity, the ratio of Weber number and gas Reynolds number ($We/Re_g = \eta_g u_{gs}/\sigma$). Here $\dot{m}_l$ is the liquid mass flux, D_t the pipe diameter, u_{gs} the superficial gas velocity, η_l and η_g the liquid and gas viscosities, ρ_l the liquid density and σ the surface tension. From inspection of the data, Azzopardi *et al.* suggested that the first two groups might be combined as $Re_l\sqrt{On}$. As seen in figure 3†, this set of dimensionless groups brings together the data with two exceptions. The first is for larger diameter pipes (A, B) where there appears to be a systematic effect. The second exception is for liquids with viscosities 4–5 times that of water (G, I). This effect is highlighted if we consider the asymptotic value of liquid Reynolds number at high gas velocities. Figure 4 shows such values from two workers who varied liquid viscosity

†This figure contains data additional to that plotted by Azzopardi *et al.* (1983). It also uses a more usual definition of Reynolds number, one four times that used in the original plot.

Table 1. Sources of data on disturbance wave inception

Identifier	Source	Pipe diameter (m)	Surface tension (kg/s^2)	Liquid	
				Density (kg/m^3)	Viscosity (kg/ms)
A	Azzopardi *et al.* (1983)	0.125	0.073	1000	0.001
B	Martin (1983)	0.058	0.073	1000	0.001
C	Whalley *et al.* (1977) Azzopardi *et al.* (1979) Shearer (1964)	0.032	0.073	1000	0.001
D	Shearer (1964)	0.016	0.073	1000	0.001
E	Asali (1984)	0.042	0.073	1000	0.0011
F		0.042	0.073	1050	0.00185
G		0.042	0.073	1150	0.0044
H	Hall Taylor and	0.0254	0.065	1000	0.0012
I	Nedderman (1968)	0.0254	0.066	1189	0.005
J		0.0254	0.067	1226	0.0105
K		0.0254	0.063	1255	0.0162
L		0.0254	0.063	1255	0.0244
M	Shearer (1964)	0.016	0.018	~1000	~0.001
N	Hall Taylor and	0.0254	0.065*	1000	0.001
O	Nedderman (1968)	0.0254	0.035*	1000	0.001

* Values cited by authors.

systematically, Hall Taylor and Nedderman (1968) and Asali (1984). The plot seems to indicate different relationships at viscosities above and below 0.007 kg/ms. Although there is a reasonable range of liquid viscosity, surface tension and pipe diameter covered in table 1, all the experiments were carried out at or near atmospheric pressure. Data sets N and O refer to aqueous solutions of surfactants used to provide lower surface tension. The authors note that surfactants alter other surface properties. In addition, as the surface tension depends on the concentration of the surfactant at the surface, the low surface tension will only be correct at that new surface if the time constant for the diffusion process is smaller than the characteristic time for the deformation process (Addison 1945). Because of this, data sets N and O have been plotted (figure 3) using the surface tension of pure water. At the high gas velocity asymptote, the critical liquid mass flux can be described by

$$\dot{m}_{lFC} = 8\left(\frac{\eta_l^2 \rho_l \sigma}{D_t^3}\right)^{1/4}. \qquad [1]$$

It was indicated earlier that there was a strong link between the inception of waves and the inception of entrainment. The latter has been considered by Ishii and Grolmes (1975), who suggest that there are two asymptotic limits of gas and liquid flow rates, as illustrated in figure 5.

There have been a number of models and correlations developed for the critical liquid flow rate for the inception of entrainment. Ishii and Grolmes (1975) suggested that the physical

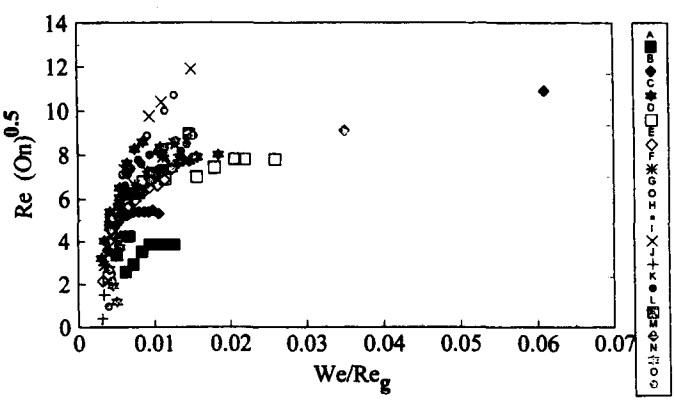

Figure 3. Plot of conditions for inception of disturbance waves. (Based on figure from 1st Int. Conf. on Physical Modelling of Multiphase Flow, Azzopardi *et al.*, "Annular two-phase flow in large diameter pipes", pp. 267–282, Copyright (1983), with kind permission of BHRA Fluid Engineering, Cranfield, UK.)

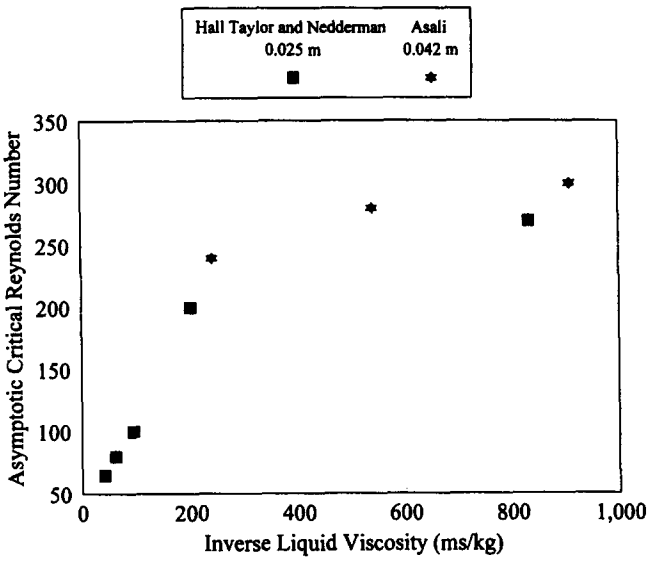

Figure 4. Effect of inverse liquid viscosity on high gas Reynolds number asymptote for wave inception.

phenomenon responsible for the start of entrainment is the penetration of the boundary layer of the gas. They proposed a critical liquid Reynolds number

$$Re_{\mathrm{lFC}} = \left(\frac{y^+}{0.347}\right)^{1.5}\left(\frac{\rho_\mathrm{l}}{\rho_\mathrm{g}}\right)^{0.75}\left(\frac{\eta_\mathrm{g}}{\eta_\mathrm{l}}\right)^{1.5}, \qquad [2]$$

where, y^+, the non-dimensional distance from the wall, takes a value of 10 and ρ_g is the gas density. Abolfadl (1984) linked the start of entrainment with onset of turbulence in the film. This he specified as a Reynolds number of 268 based on available experimental data. Asali *et al.* (1985) used an analysis of the stability of disturbance waves on the interface to determine that the critical liquid Reynolds number for their inception, and hence entrainment, depended on the group $(\eta_\mathrm{l}/\eta_\mathrm{g})\sqrt{(\rho_\mathrm{g}/\rho_\mathrm{l})}$. They provided a graphical correlation between this and the critical Reynolds number. Owen and Hewitt (1984) modified this correlation to account for evaporation of the film and obtained

$$Re_{\mathrm{lFC}} = \mathrm{e}^{5.8405+0.4249(\eta_\mathrm{g}/\eta_\mathrm{l})\sqrt{(\rho_\mathrm{l}/\rho_\mathrm{g})}}. \qquad [3]$$

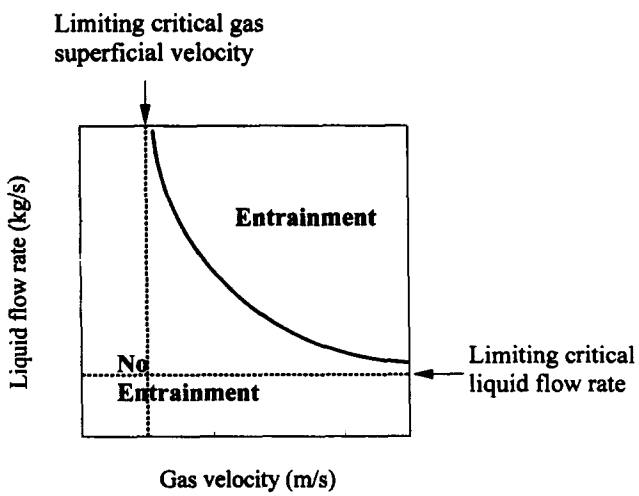

Figure 5. Typical plot marking conditions for entrainment.

Table 2. Critical liquid Reynolds number for wave inception at high gas velocity

Source	Experimental	Abolfadl (1984)	Asali (1984)	Owen and Hewitt (1984)	Ishii and Grolmes (1975)
A	211	268	290	429	58
B	245	268	272	412	43
C	330/360	268	284/272	423/412	53/43
D	255	268	284	423	53
E	300	268	272	411	46
F	282	268	231	383	22
G	240	268	225	261	7
H	205	268	225	345	40
I	205	268	225	359	5.4
J	105	268	225	351	1.8
K	90	268	225	348	1
L	70	268	225	347	0.5
M		268			
N	272	268	284	423	53
O	298	268	284	423	53

The above methods have been tested against the wave inception data from the sources listed in table 1. In each case the asymptotic liquid Reynolds number at high gas flow rate was deduced. These values are tabulated in table 2 together with the equivalent predictions of [1]–[3]. There are obvious trends with pipe diameter and liquid viscosity. None of the prediction methods include the effect of pipe diameter. For viscosity, the Asali *et al.* (1985) and Owen and Hewitt (1984) methods do not give a strong enough trend whilst Ishii and Grolmes (1975) have too strong a trend. It can be seen that the absolute values predicted by Ishii and Grolmes are too low. This could be rectified by using a value of y^+ of say 30.

Nigmatulin *et al.* (1996) suggests an alternative expression for the critical Reynolds number. This is based on a Weber number, the ratio of interfacial shear stress times film thickness to surface tension.

Willetts (1987), examining the critical flow rate for inception of entrainment, commented that, because of the uncertainties in measurement, it was not possible to recommend Asali *et al.* (1985) or Owen and Hewitt (1984) above the other. He noted that there appeared to be a significant viscosity effect and a small surface tension effect not accounted for by either method. It is seen above that the correlation of Azzopardi *et al.* (1983) shown in figure 3 draws together most of the data on wave inception onto a single curve. Hills (1997) has tested the suitability of the curve to predict the critical liquid flow rate for the inception of entrainment including recent data. The experimental values were obtained in a number of ways: (i) following the suggestion of Schadel *et al.* (1990), the entrained liquid flow rate was plotted against the total liquid flow rate and the intercept at zero determined entrained liquid; (ii) taken directly from the values reported by Fore and Dukler (1995a) who determined the critical flow rate as that value, when increasing the liquid flow rate, at which drops were first observed; and (iii) from the data of Asali *et al.* (1985) which were obtained by increasing the gas flow for a fixed liquid flow, and measuring the resulting film mass flux—this reached a maximum value at high gas rates, which was taken as the critical liquid flow rate. These data have been compared against the wave inception data. The results are shown in figure 6 on the same axes as figure 3. Most of the data show the same trend as that for wave inception. It is interesting to note that the data on critical liquid flow rate for entrainment from the data of Azzopardi *et al.* (1983) are similar to most other data, even though the wave inception data is lower than that for smaller diameter pipes.

For the limiting gas velocity, Ishii and Grolmes (1975) proposed that, at low liquid flow rates, the mechanism of entrainment changes from one based on shear to an undercutting of the wave. They argued that the latter could be well correlated by a Weber number based on the film thickness. This results in

$$\frac{\eta_l u_{gsC}}{\sigma}\sqrt{\frac{\rho_g}{\rho_l}} \geq \frac{1.5}{Re_l}. \qquad [4]$$

Jepson (1992) has tested this equation against a variety of fluids (mainly in 0.01 m diameter pipes). Figure 7 shows that this equation appears to underpredict the critical gas velocity for

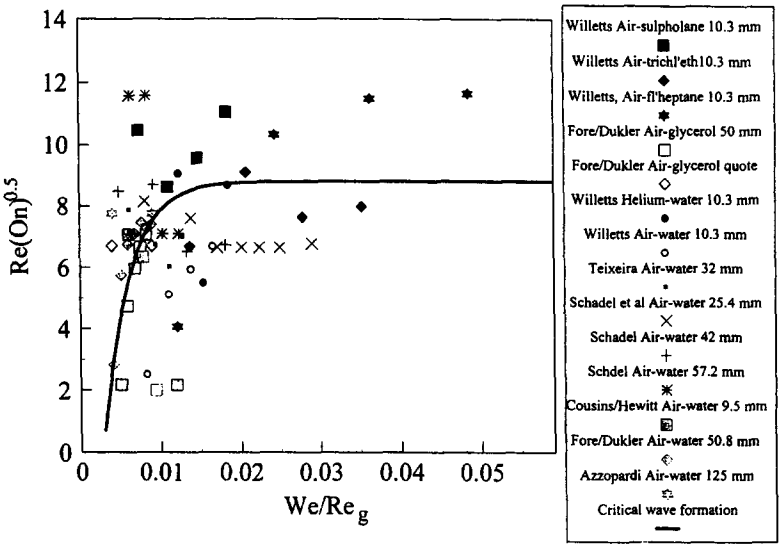

Figure 6. Plot of conditions for inception of entrainment on same axes as suggested for wave inception by Azzopardi *et al.* (1983). (Based on figure from 4th World Congress on Experimental Heat Transfer, Fluid Mechanics and Thermodynamics, Vol. 2, Hills, "The critical liquid flow rate for wave and droplet formation in annular gas-liquid flow", pp. 1241–1247, Copyright (1997), with kind permission of Edizioni ETS s.r.l., Pisa.)

inception of entrainment. However, figure 6 brings into question whether the asymptote is towards a high liquid flow rate as indicated in figure 5 or a low liquid flow rate.

2.2. *Properties of disturbance waves*

The properties of disturbance waves have been measured by one of two methods. The first was from cine films taken through the transparent pipe wall. The second type used continuous film thickness records. In the latter case the frequency was obtained from autospectrum and the velocity was obtained from the cross spectrum of film thicknesses records taken at two axial positions.

As mentioned above, for vertical upflow in small diameter pipes, disturbance waves appear as coherent milky bands travelling faster than the film. Figure 8a illustrates such a wave from a 0.032 m diameter tube. Supporting evidence for the circumferential coherence is provided by the

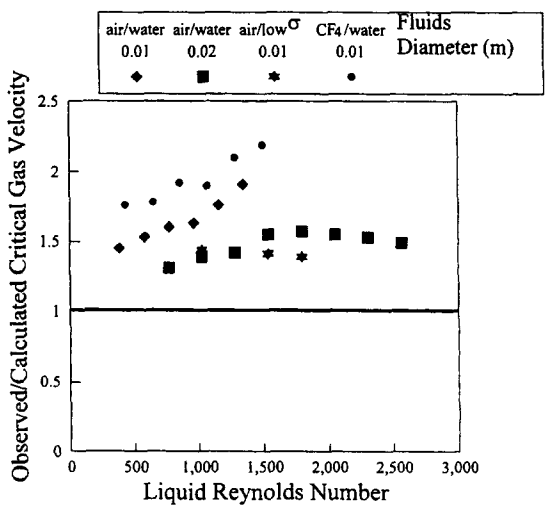

Figure 7. Test of equation of Ishii and Grolmes (1975) for critical gas flow rate for inception of entrainment.

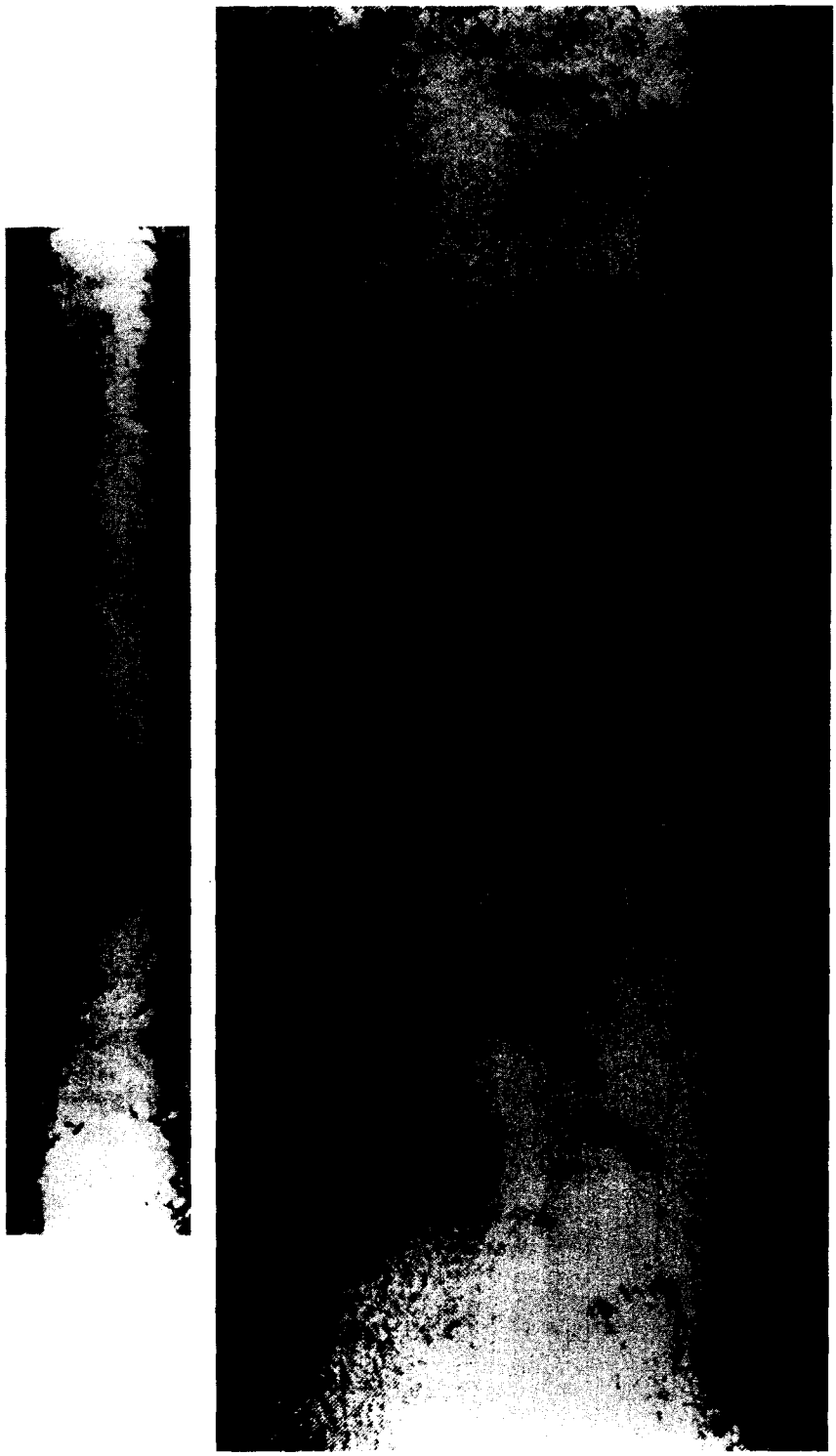

Figure 8. Photographs of disturbance waves in vertical upward annular flow: (a) 0.032 m diameter tube; (b) 0.125 m diameter tube. (Reproduced from The Chemical Engineer, No. 398, Azzopardi and Gibbons, "Annular two-phase flow in a large diameter tube", pp. 19–31, Copyright (1983), with kind permission of the I. Chem. E., Rugby, UK.)

work of Hewitt and Lovegrove (1969) who made simultaneous measurements of film thickness at four points uniformly placed around a 0.032 m diameter tube at one axial location. Waves appeared as simultaneous increases in the four film thickness signals, although the peak height was not uniform on all four signals. Thus, in this size of tube, the wave shows reasonable

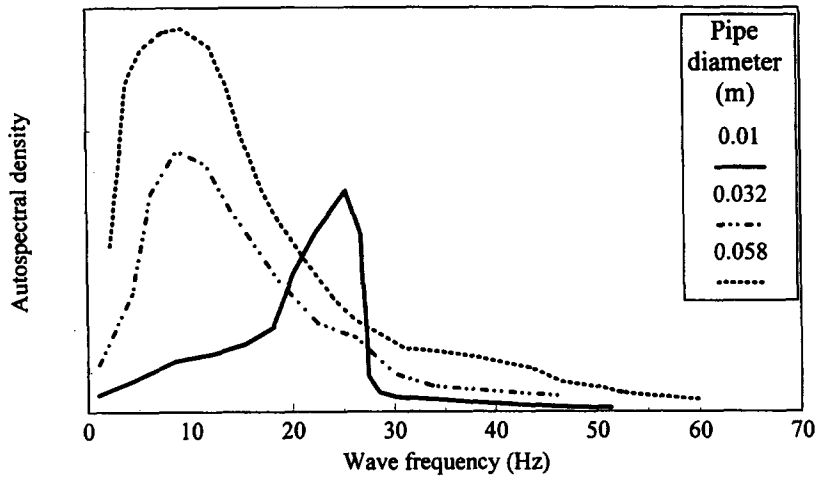

Figure 9. Autospectral densities of film thickness measurements—effect of tube diameter (Martin and Azzopardi 1985).

coherence. However, in a 0.125 m diameter tube, Azzopardi *et al.* (1983) have observed that waves are circumferentially localized (figure 8b). Here the waves are curved, parts being further downstream than others. Observations made by Martin and Azzopardi (1985) indicate that this breakdown in coherence is systematic. For a 0.01 m diameter pipe the waves could be described as highly regular about the pipe. In the case of a 0.058 m diameter pipe, the waves were less clear cut, having circumferential completeness only for certain flow rates. Quantitative illustration of the coherence can be found in the autospectral density of film thickness signals. A large degree of coherence will manifest itself as a very sharp-peaked version of this function. Figure 9 shows autospectral densities measured on 0.01, 0.032 and 0.058 m diameter pipes. The broadening with diameter is indicative of a decrease in the degree of coherence. Recently, Okada *et al.* (1995) have provided evidence that the lack of coherence could extend to smaller diameters if the gas velocity was high enough. They identified two types of waves, two-dimensional disturbance waves (classified as DW1) and three-dimensional disturbance waves (DW2). DW1 were described as having crests perpendicular to the tube axis and coherent about the tube circumference, whereas DW2 were formed obliquely to the tube axis. A part of the ring wave begins to be broken and these waves do not have coherence about the tube circumference. It is interesting that the combined frequency of DW1 and DW2 are in reasonable agreement

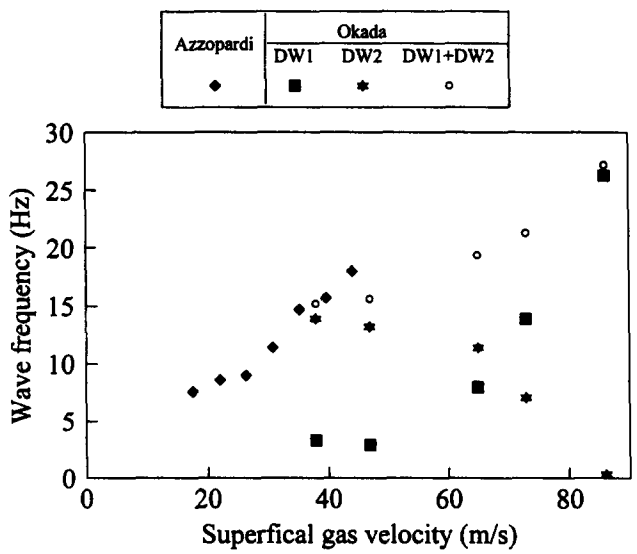

Figure 10. Frequencies of DW1 and DW2 waves as identified by Okada *et al.* (1995).

Table 3. Sources of data on disturbance wave properties in vertical upflow

Source	Pipe diameter (m)	Pressure (bar)	Superficial velocity (m/s)		Parameters measured
			Gas	Liquid	
Hall Taylor *et al.* (1963)	0.032	1.1–1.3	15–27	0.01–0.033	*c*, *f*
Nedderman and Shearer (1963)	0.032	1.1–1.2	14–75	0.011–0.23	*c*, *f*
	0.016	1.1–1.4	15–88	0.021–0.31	*c*, *f*
Gill *et al.* (1969)	0.032	2–44	20–40	0.032	*c*
Hewitt and Lovegrove (1969)	0.032	1.1–2.2	16–43	0.016–0.32	*c*, *f*
Pashniak (1969)	0.025[a]	2	14–32	0.0005–0.01	*c*
Sekoguchi *et al.* (1973)	0.025	~1	15–36	0.013–0.048	*c*, *f*
Tomida and Okazaki (1974)	0.01	1	2–63	0.128–0.91	*c*, *f*
Whalley *et al.* (1974)	0.032	2.75	14–43	0.016–0.11	*c*, *f*
Brown *et al.* (1975)	0.0096[1]	~1	50–250	0.15–0.17	*c*, *f*
Brown (1978)	0.032	2.4–3.4	18–39	0.08–0.16	*c*, *f*
Wurtz (1978)	0.02[1]	70	2.7–22	0.2–2.13	*c*, *f*
Azzopardi (1986)	0.032	1.5	17.6–44	0.016–0.16	*c*, *f*
Martin (1983)	0.01	1.5	22.2-44.4	0.04-0.1	*c*, *f*
	0.032	1.5	11.1-55.5	0.04-0.08	*c*, *f*
	0.058	1.5	11.1-33.3	0.02–0.06	*c*, *f*
Willetts (1987)	0.01	1.5	11.1-66.6	0.02-0.14	*c*, *f*
	0.01[2]	1.5	22–73	0.02–0.14	*c*, *f*
Schadel (1988)	0.025	1.1	32.2-90.6	0.019-0.1	*c*, *f*, *I*
	0.042	1.3	19.5–71.8	0.15–0.067	*c*, *f*, *I*
Sawai *et al.* (1989)	0.004[1]	29.5	10.3-32.6	0.016-0.32	*c*, *f*
	0.005	1, 3, 5.4	23.7–38.3	0.03–0.25	*c*, *f*
Ohba and Nagae (1993)	0.029	~1	14–31	0.0063–0.038	*c*, *f*
Wolf (1995)	0.032	1.3–2.4	24–95	0.01–0.12	*c*, *f*
Okada *et al.* (1995)	0.03	~1	28–102	0.012–0.146	*f*

[a] Steam/water; [b] Helium/water. *c* = wave velocity; *f* = wave frequency; *I* = intermittency.

with the data of Azzopardi (1986), even though that for DW1 falls and that for DW2 rises with increasing gas velocity (figure 10).

The frequency and velocity of waves have been determined for a number of pipe diameters and flow rates. The sources and ranges of flow rates are given in tables 3 and 4 for vertical upflow and horizontal flow. There are a number of data sets for vertical downflow. Many of these are for falling film flows with no gas flow. Two-phase flow data has been published by, e.g., Thwaites *et al.* (1976) and Webb and Hewitt (1975). It is noted that, in all orientations, the majority of the data are for pipes of about 0.03 m at near atmospheric pressures. Only five of the sources use fluids other than air and water.

The following trends have been observed in the frequency data:

1. Frequency increases with both gas and liquid flow rates (Nedderman and Shearer 1963; Hall Taylor *et al.* 1963).
2. Frequency decreases with distance downstream when the liquid is introduced as a film (Hall Taylor and Nedderman 1968; Gill *et al.* 1969). This decrease is due to the disturbance wave coalescing, two joining to form one, and can be accounted for by theories based on the probability distribution of velocities (Hall Taylor and Nedderman 1968; Wilkes *et al.* 1983a). Where the annular flow is created by evaporation of liquid to vapour in the tube, the frequency does not vary with axial position (Sawai *et al.* 1989).
3. Frequency increases with gas density for a given gas velocity (Gill *et al.* 1969).
4. Frequency is independent of gas volume upstream of liquid inlet (Gill *et al.* 1969), so there is no sounding box effect.
5. The frequencies measured by different workers for the same nominal conditions show differences of up to 60% (Hall Taylor *et al.* 1963; Nedderman and Shearer 1963; Hewitt and Lovegrove 1969; Azzopardi 1986). These differences are probably due to the experimental techniques employed.
6. For vertical downflow, the frequency is independent of gas flow rate for low gas rates but shows an (approximately) linear dependence at higher gas flow rates, e.g. Thwaites *et al.* (1976).

Table 4. Sources of data on disturbance wave properties for stratified/annular flow in horizontal tubes

Source	Pipe diameter (m)	Pressure (bar)	Superficial velocity (m/s)		Parameters measured
			Gas	Liquid	
Pearce (1979)	0.032	1–1.28	24–55	0.03–0.5	*c*
Fukano *et al.* (1983)	0.026	1–1.28	10–55	0.0006–0.4	*c*, *f*
Jayanti *et al.* (1990)	0.032	1.61–2.43	14.3–25.7	0.08–0.145	*c*, *f*
Paras and Karabelas (1991)	0.05	1.08	30–66	0.02–0.2	*c*, *f*, *I*
Andritsos (1992)	0.095	1.25	3.4–14.4	0.0095–0.107	*c*, *f*
Paras *et al.* (1994)	0.05	1.08	11–65.4	0.019–0.2	*c*, *f*, *I*

Shearer (1964) has suggested that the wave frequency could be correlated through a Strouhal number (fD_c/u) and a liquid Reynolds number. The gas velocity, u, was specified as that between the disturbance waves with the diameter, D_c, being that of the gas core in the same position. Examination has shown that use of the superficial gas velocity and pipe diameter makes little difference to the Strouhal number. This is now defined as (fD_t/u_{gs}). It is suggested that the Reynolds number defined by Shearer is replaced by an excess Reynolds number, i.e. one based on the film flow rate over and above the critical film flow rate for wave inception. There are two reasons for this. Firstly, if the Reynolds number defined by Shearer is used, the data does not lie on straight lines on a logarithmic plot, using the excess Reynolds number does give straight lines. Secondly, as will be seen below, correlations for the rate of entrainment employ excess film flow rates. The data from the sources in table 3 have been recalculated in this manner. The data for the air–water experiments are plotted in figure 11. This approach brings together data whose frequencies would normally have covered two orders of magnitude. However, before this approach is developed any further, more accurate prediction methods are required for the critical film flow rate. Data from the 0.058 m diameter pipe have been omitted as they were measured only 50 diameters from the inlet and so the frequency might not have decreased from the inlet value to the lower value caused by coalescence of the waves.

For wave velocity, the following trends were deduced:

1. Disturbance wave velocities increase with both gas and liquid flow rates (Hall Taylor *et al.* 1963; Nedderman and Shearer 1963; Azzopardi 1986). However, the effect of gas is greater than that of the liquid.
2. There is a small increase in wave velocity along the tube when the liquid is introduced as a film but a steady state is soon achieved (Gill *et al.* 1969; Brown 1978). When the annular flow is created is by the evaporation of part of the liquid in the tube, there is very little change in the velocity in the downstream section where there is no heating (Brown *et al.* 1975; Sawai *et al.* 1989).

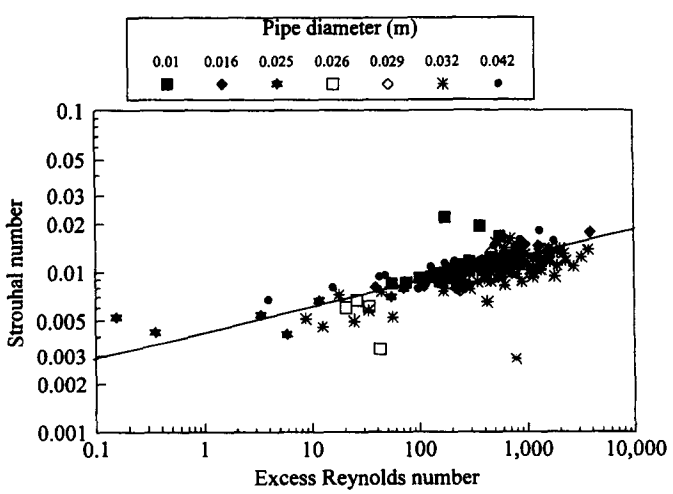

Figure 11. Correlation of wave frequency data following suggestions of Shearer (1964).

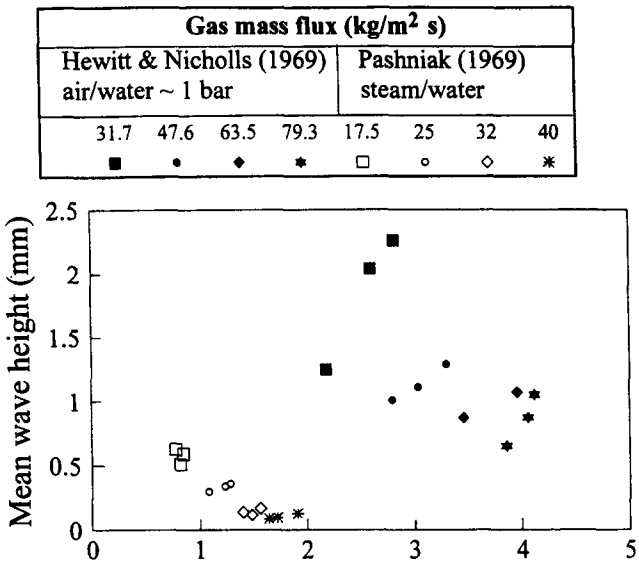

Figure 12. Effect of wave height on wave velocity.

3. Velocity decreases with gas density to the power of 0.3 (Gill *et al.* 1969; Hewitt and Lovegrove 1969).
4. Individual velocities are normally distributed about a mean (Hall Taylor *et al.* 1963), and the absolute standard deviation tends to be constant (Hall Taylor 1967).
5. Wave velocities depend linearly on wave height. Pashniak (1969) has shown this to be approximately correct for individual waves. The mean value results of Pashniak and Hewitt and Nicholls (1969), are shown in figure 12 where it can be seen that the level of linearity for individual data sets is quite high.
6. In horizontal flow, the wave velocity was found to be higher at the top than at the bottom (Jayanti *et al.* 1990).

Methods for correlating wave velocities have been suggested by Pearce (1979), Sawai *et al.* (1989) and Paras *et al.* (1994). Pearce, working with horizontal annular flow, proposed that the wave velocity was described by a combination of the film and gas velocities. Sawai *et al.* correlated their own vertical upflow data against friction velocity (based on the interfacial friction equation of Henstock and Hanratty, 1976) for air–water data and against the ratio of interfacial shear stress to mass flux for steam–water data. In both cases the relationship determined was linear with an intercept of zero. Paras *et al.*, who were working on horizontal stratified/annular flows, correlated wave velocities against the group $G = (u_{gs}^5 h_0/D_t)^{0.5}$, where h_0 is the wave height at the tube bottom. They suggested an equation of the form $v_w = 0.75 + 0.002G$. When compared with the data from the sources in table 3, the velocity groups proposed by Pearce and Sawai *et al.* did not correlate the entire database. However, the group of Paras *et al.* showed some correlation, although their equation, proposed for horizontal flow, did not apply to this vertical flow data, as shown in figure 13. Instead, wave velocities appear to approach an asymptotic upper limit. For horizontal stratified/annular flow the equation suggested by Paras *et al.* gives reasonable agreement with the data, figure 14. This includes data by Pearce (1979) and Jayanti *et al.* (1990) not considered by Paras *et al.*

It has been suggested that the wavelength (or more correctly the spacing between the waves, i.e. the ratio of velocity to frequency) could be an important parameter in the prediction of pressure drop. More particularly one might expect that the wave height would also influence pressure drop. Although there is very little information on wave heights, Hewitt and Nicholls (1969) have suggested that this parameter has values five times the mean film thickness. Wave spacing over film thickness has been plotted against a Reynolds number based on the excess liquid flow rate over that for the inception of entrainment. This definition has been chosen for

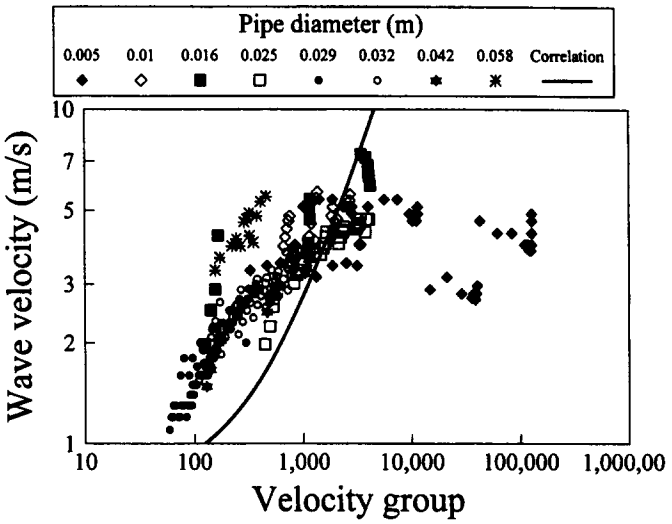

Figure 13. Correlation of wave velocity data for vertical upflow against dimensional group suggested by Paras *et al.* (1994).

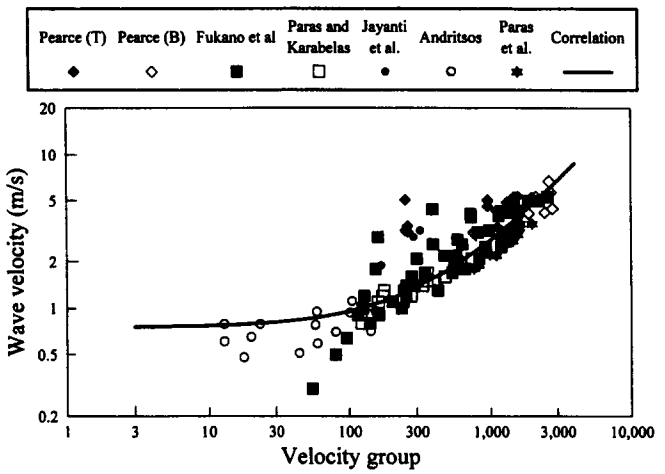

Figure 14. Correlation of wave velocity data for horizontal stratified/annular flow against dimensional group suggested by Paras *et al.* (1994).

reasons similar to those put forward for frequency. Figure 15† this shows air–water data. Although there is a trend with tube diameter, there appears to be a dependence on the excess liquid Reynolds number to the power of $-1/4$.

Another property of waves which is important for the process of drop creation is the intermittency—the fraction of the film surface covered by waves. Its use was first proposed by Tatterson (1975) who was attempting to apply the analysis suggested by Taylor (1940), but appreciated that the surface of the film was not all covered by waves. It has been determined for vertical upflow by Schadel (1988) and for horizontal flow by Paras *et al.* (1994). Their results are illustrated in figure 16. As can be seen the intermittency decreases with gas velocity in vertical flow but increases to a fairly constant value in horizontal flow. Schadel (1988) showed that the intermittency increases with the excess liquid flow rate (over the critical value for inception of entrainment) and showed no effect of tube diameter. However, the data show different trends with gas velocity for the vertical and horizontal flow cases.

†The film thickness was calculated using the equation of Ambrosini *et al.* (1991) and the critical liquid flow rate by the equation of Owen and Hewitt (1984).

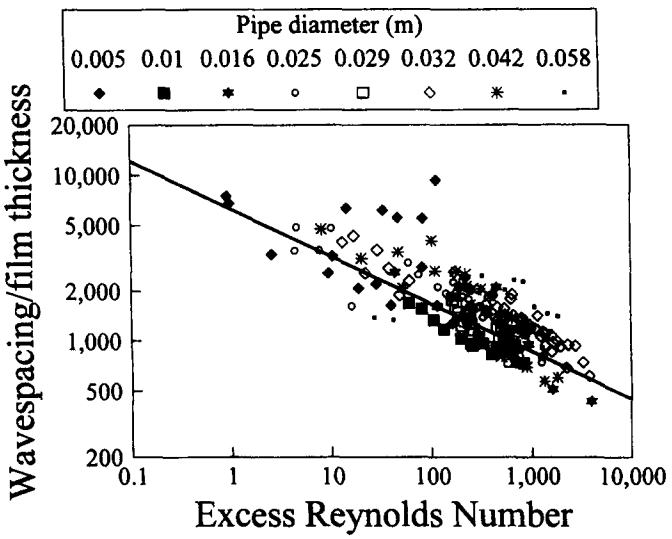

Figure 15. Correlation of wave spacing/film thickness.

2.3. *Huge waves*

The occurrence of huge waves was identified by Sekoguchi at Osaka (Sekoguchi and Takeishi 1989; Sekoguchi and Mori 1997). Their experiments employed very extensively instrumented test

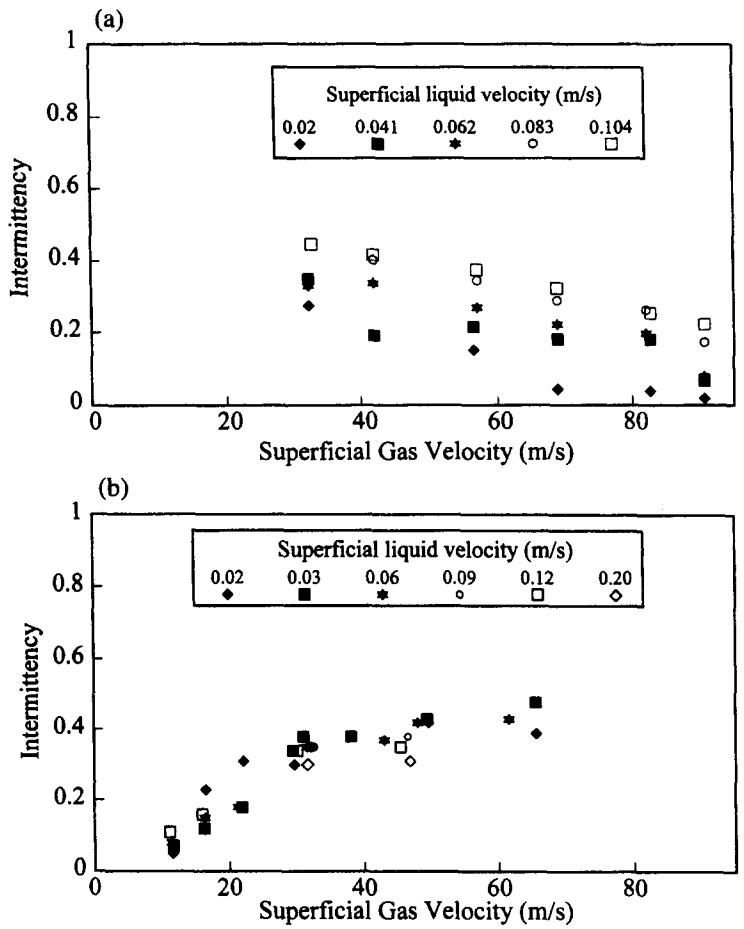

Figure 16. Intermittency of disturbance waves: (a) vertical upflow (Schadel and Hanratty 1989); (b) horizontal flow (Paras *et al.* 1994).

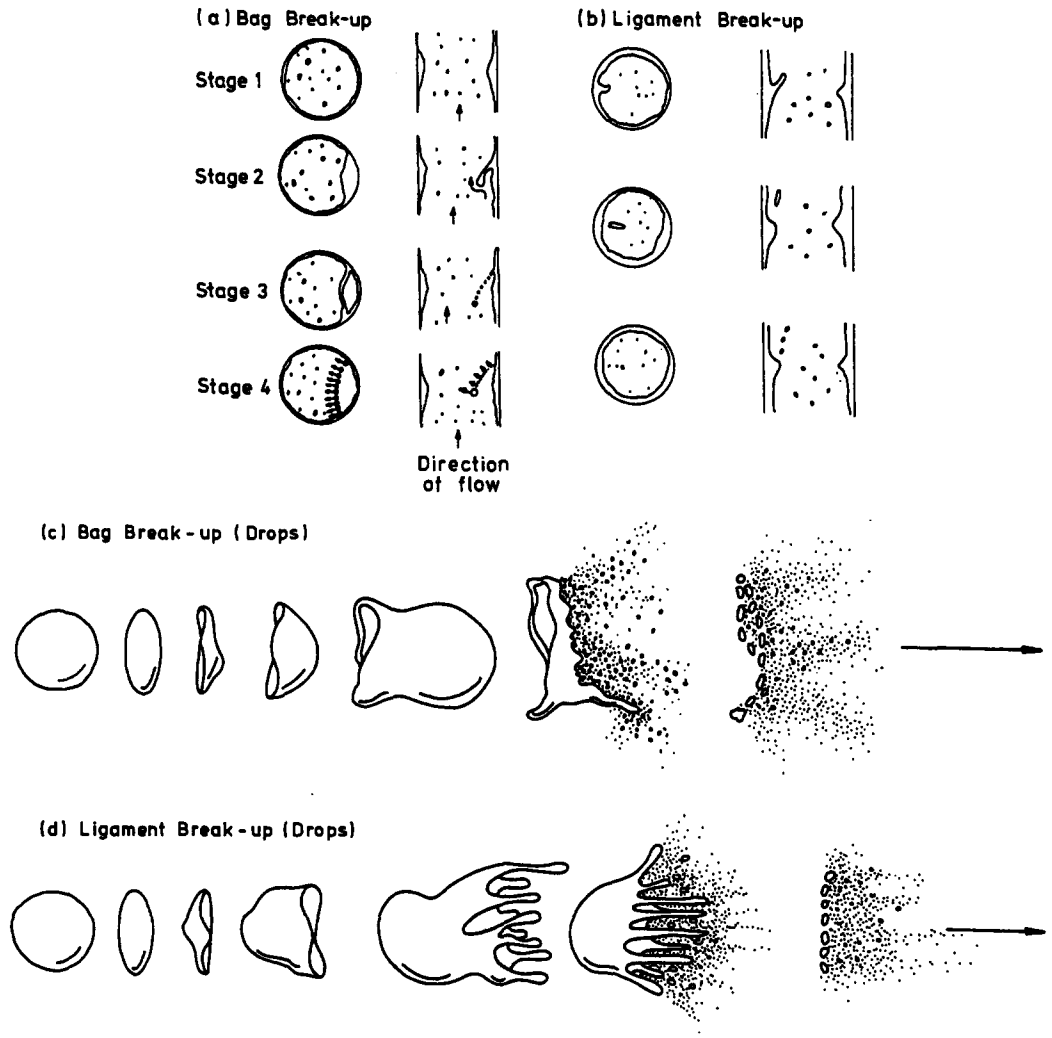

Figure 17. Mechanisms of atomization and drop break up. (Reproduced from UKAEA Report AERE R-11068, Azzopardi, "Mechanisms of entrainment in annular two-phase flow", Copyright (1983), with kind permission of AEA Technology plc., Harwell, UK.)

sections which provided time–space data of film thicknesses. Those records showed that, in addition to disturbance waves, there were other, larger amplitude waves with longer wavelengths and larger velocities. These were termed huge waves, they could co-exist with disturbance waves for some conditions and they occurred at higher liquid flow rates and lower gas flow rates—extending into the wispy-annular and churn flow regimes. Interestingly, the velocities of these huge waves appear similar to those of waves measured by Hawkes and Hewitt (1995) in wispy-anular flow. However, they are slower than the wisps, the form in which the entrained liquid is travelling at higher liquid flow rates. Obviously, there is a need to understand details of wispy-annular flow.

2.4. *Mechanisms of atomization*

Azzopardi (1983) used an axial viewing technique to examine the mechanisms of atomization in vertical upflow. Two different mechanisms were identified. The first, termed bag break-up, occurred at lower gas and liquid flow rates and is illustrated in figure 17. Part of the disturbance wave is undercut and a open-ended bubble is formed with a thick filament rim. Gas pressure builds up within the bubble or bag causing it to expand and eventually burst. This forms a number of small drops whilst the rim breaks up shortly afterwards giving a smaller number of larger drops. A similar mechanism had been reported earlier by Woodmansee and Hanratty (1969) for

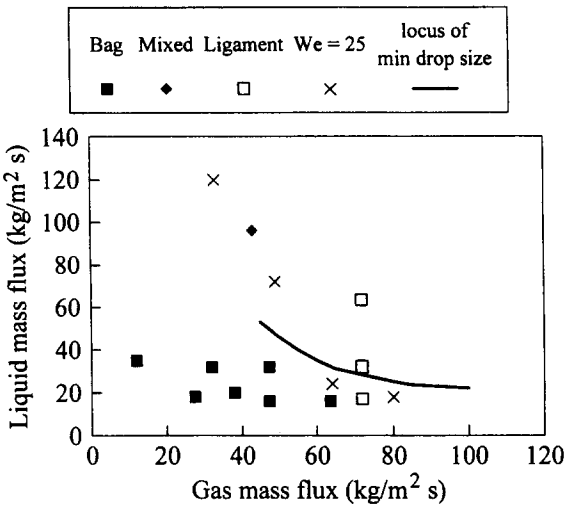

Figure 18. Transition between bag and ligament mechanisms of entrainment. (Based on figure from UKAEA Report AERE R-11068, Azzopardi, "Mechanisms of entrainment in annular two-phase flow", Copyright (1983), with kind permission of AEA Technology plc., Harwell, UK.)

horizontal flow. At higher flow rates, Azzopardi (1983) reported that a second mechanism occurred in which the crests of roll waves were elongated and thin ligaments were torn from the film. These ligaments immediately broke down into drops. These mechanisms are similar to those which occur when large drops are distorted and broken up by the effect of a gas stream. Azzopardi proposed that, as for drop break-up, the boundary between the mechanisms can be described by a Weber number using the wave height as the length scale. Figure 18 shows that this described the boundary reasonably accurately. The bag break-up mechanism has been considered to be the most important. However, figure 18 shows that the ligament mechanism is relevant over greater ranges of flow rates. Moreover, bag break-up occurs at lower gas velocities, those that are easier to observe.

2.5. *Measurement of the rate of entrainment*

It is not easy to make measurements of a complex process such as entrainment from the film into the gas core. In the case of deposition, unidirectional experiments can be carried out such that entrainment is not occurring. No such simple scheme is available for measuring entrainment rates. It is not possible to remove the drops from the gas core without causing significant disturbance to the flow. Equally, it is not possible to get close to the source of the entrainment, namely the disturbance waves from which the drops are created, primarily because they are moving along the tube. Estimates of entrainment rate, based on the initial rates of entrainment immediately after the creation of the liquid film, can be very misleading. This is because the flow is developing and quite some distance is required before disturbance waves are formed and develop some sort of equilibrium.

One method of determining the rate of entrainment uses a mass balance on an element of liquid film. This yields

$$\frac{d\dot{m}_{lF}}{dz} = \frac{4}{D_t}(R_D - R_A), \qquad [5]$$

where $\dot{m}_{lF}$ is the liquid film mass flux, z is the axial coordinate and R_D and R_A are the rates of deposition and entrainment respectively. Hutchinson and Whalley (1973) considered hydrodynamic equilibrium, i.e. when the rate of change of film flow rate is zero and the rate of entrainment equals the deposition rate. Measurement of the drop flow rate can yield a rate of deposition and hence a rate of entrainment. In contrast, Ueda (1979) and Wilkes *et al.* (1983a) made measurements in flows where equilibrium had not been reached. They measured the film flow rate at different points along the tube and hence obtained the gradient $d\dot{m}_{lF}/dz$. This, together with a description of the rate of deposition can be used to provide a measure of the

rate of entrainment. As the gradient is determined from the small difference between two film flow rates, any errors in measurement of film flow rate would be magnified.

A disadvantage of using the approaches described above is that they involve two unknowns, R_D and R_A, and only one equation. If a tracer were injected into the film at a known concentration, the concentration would diminish because of removal of some tracer by entrainment and deposition of tracer-free liquid by deposition. Measurements can be made of the concentration in the film at different distances from the injection point. A mass balance on the tracer

$$\frac{d(\dot{m}_{lF}c_F)}{dz} = \frac{4}{D_t}(R_D c_A - R_A c_F), \qquad [6]$$

where c_F is the concentration in the film and c_A is the tracer concentration in the entrained liquid. The mixing cup concentration can be defined as $c_e = c_F(1 - E) + c_A E$ and relating this to the initial conditions $c_e = c_{F0}(1 - E_0)$, where E is the fraction of liquid entrained. Using these, [5] and [6] can be combined to give

$$\frac{d(\ln p)}{dz} = \frac{4R_D}{\dot{m}_l D_t}[E(1 - E)]^{-1}, \qquad [7]$$

where $p = c_F/c_e - 1$ and thence R_A is determined from the rate of change of film flow rate, [5].

This approach was first proposed by Quandt (1965) and versions used by Jagota *et al.* (1973), Andreussi and Zanelli (1978) and Andreussi (1983). The equations as given above were produced by Leman *et al.* (1985) and have also been used by Schadel (1988), Schadel and Hanratty (1989) and Schadel *et al.* (1990). Examples of the results obtained by Leman *et al.* are shown in figure 19.

A completely different approach has been suggested by Azzopardi and Whalley (1980). This starts from the identification of disturbance waves as the sources of entrainment. If the flow can be arranged so that there is only one wave in the tube at a time, say by injecting a small volume of liquid into a film flow set at the critical value for wave inception, then the source of entrainment, though moving, is clearly identified. Measurement of the flux of entrained liquid whilst the wave is travelling up the tube gives values which increase as the wave approaches the measuring station. Obviously, the further the wave is from the measuring station the further the drops have travelled and the more chance there is for deposition to take place. If the drop flow rate is measured when the wave is almost at the measuring station, this value is nearest to the entrained flow rate and can be converted to the rate of entrainment if the appropriate area is employed. Azzopardi and Whalley (1980) took high speed cine films through an axial viewer

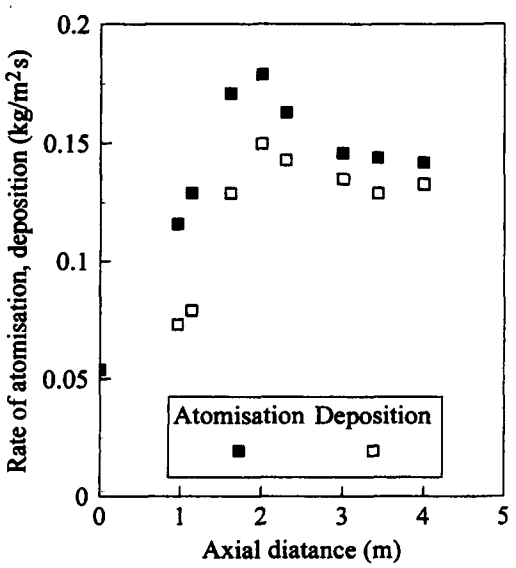

Figure 19. Measured rates of entrainment and deposition using tracer technique (Leman *et al.* 1985).

and determined the entrained liquid flow rate via analysis of individual frames. This process was tedious, time consuming and not very accurate. Subsequently, Gibbons *et al.* (1985) employed a laser anemometry technique to count and size the drops. The results are difficult to obtain and interpret. However, they have given independent confirmation of data obtained by other methods.

2.6. *Equations for entrainment rate*

Here, published equations which predict the rate of entrainment are covered briefly. The objective here is to show the link with the parameters discussed in this paper. The first approach to predict the rate of entrainment used the concept of equilibrium in the entrainment/deposition process and assumed a similarity between the equation for the two processes. Hutchinson and Whalley (1973) determined that the equilibrium concentration could be correlated by a form of Weber number ($\tau_i\delta/\sigma$, where τ_i is the interfacial shear stress and δ is the film thickness). The concentration when multiplied by the mass transfer coefficient (taken to be equal to that for deposition) resulted in the rate of entrainment. Later work correlated the rate of entrainment directly. In most cases, allowance was made for a critical liquid flow rate below which there were no disturbance waves and thence to entrainment (Leman *et al.* 1985; Govan *et al.* 1988; Schadel *et al.* 1990). The entrainment rate was described as linearly dependent on gas velocity and having a power law dependence on excess liquid flow rate with values of the power of 0.632 and 1 being suggested. Extra terms to account for additional mechanisms have been proposed by Miloshenko *et al.* (1989), effect of evaporation, and Nigmatulin (1991), effect of the shocks produced by depositing drops striking the film.

Schadel and Hanratty (1989) have started to involve wave intermittency in the prediction of rate of entrainment. However, as there are only limited data on intermittency, this approach does not yet have wide application.

Although, at higher gas velocities, the fraction of liquid obtained increases with gas velocity, at lower gas velocities, probably towards the churn flow boundary, the opposite has been found (Verbeek *et al.* 1992; Azzopardi 1994). This needs to be explored further.

3. CONCLUSIONS ON WAVES AND DROP CREATION

From the above it can be concluded that:

1. Drops are created from disturbance waves as shown by the artificial wave experiments of Azzopardi and Whalley (1980). Additionally, the recent work of Hills (1997) shows that inception of disturbance waves and entrainment of liquid to form drops appear to coincide.
2. Disturbance waves are characterized by frequencies correlated by a Strouhal number, implying direct proportionality to the gas velocity. There is also a small dependence on a liquid Reynolds number based on the excess flow rate over that for wave inception. The ratio of wavelength to mean film thickness also depends on this excess Reynolds number. However, at present, this correlation is confined to air–water data. Obviously, more data is required for fluids other than air–water and for larger diameter pipes.
3. The best technique to determine rates of entrainment is the tracer technique originally proposed by Quandt (1965). The available data are very limited and further experiments covering wide ranges of parameters are required.
4. Predictive methods for the rate of entrainment are still very empirical.
5. There is a need for a theoretical basis for disturbance waves and entrainment. Progress might arise from further analysis of the available experimental data.

4. DROPS— SIZES AND VELOCITIES

4.1. *Drop size distribution and means*

It is a characteristic of the drop field in annular two-phase flow that it contains drops with a distribution of sizes. These distributions can vary in time and space. This can have important implications in any comparison between the results obtained by different measuring techniques

as they make different measurements. In particular, the laser diffraction technique (Malvern) measures an average over space and time whilst the laser Doppler methods make measurements at a point in space.

A number of equations have been used to describe the distribution of sizes in annular flow. The equation of Rosin and Rammler (1933) was originally designed to describe the distribution of mass of coal dust obtained from sieving. It is not surprising that it is written in terms of the cumulative volume in sizes greater than D

$$R = 1 - e^{-(D/\bar{X})^N}. \quad [8]$$

This can be rearranged into the usual differential form

$$v(D) = \frac{ND^{N-1}}{\bar{X}^N} e^{-(D/\bar{X})^N}. \quad [9]$$

The number distribution form can be obtained from this by dividing $v(D)$ by D^3 and inserting a factor to make $\int_0^\infty n(D)\,dD = 1$.

This yields

$$n(D) = \frac{ND^{N-4}}{\bar{X}^{N-3}\Gamma\left(1 - \frac{3}{n}\right)} e^{-\left(\frac{D}{\bar{X}}\right)^N}, \quad [10]$$

where Γ is the gamma function.

Inspection of this equation shows that for $N < 4$, the number of drops tends to infinity as the drop size tends towards zero.

A feature to be noted is that (mathematically) the Rosin–Rammler equation has no natural upper cut off, it has a tail to infinite drop sizes. Similarly, most of the other equations discussed do not have an upper limit to drop diameter. It can be argued that this is against physical reasonableness and a more suitable equation is the "upper limit log normal" (ULLN) distribution suggested by Mugele and Evans (1951):

$$v(D) = \frac{\delta}{\sqrt{\pi}} e^{-(\delta y)^2}, \quad [11]$$

where δ is a fitting parameter and y is defined as

$$y = \ln\left(\frac{kD}{D_{max} - D}\right). \quad [12]$$

D_{max} is the maximum drop diameter and k is given by

$$k = \frac{D_{max} - D_{vm}}{D_{vm}}. \quad [13]$$

D_{vm} is the volume median diameter, the diameter size below which is contained 50% of the distribution by volume. Information on the parameters k and δ in the upper limit log normal equation for annular flow data has been given by Andreussi *et al.* (1978), Kataoka *et al.* (1983), Kocamustafaogullari *et al.* (1993) and Hay *et al.* (1996). They all found similar values for these parameters. Mean values were $k = 2$ and $\delta = 0.8$.

Most drop size data are reported as a single number. Because drops of different sizes can contain significantly different mass of liquid, a simple arithmetic mean is inadequate. A commonly used mean is the Sauter mean diameter

$$D_{32} = \frac{\int_0^{D_{max}} D^3 n(D)\,dD}{\int_0^{D_{max}} D^2 n(D)\,dD}, \quad [14]$$

where $n(D)$ is the number of drops of size D.

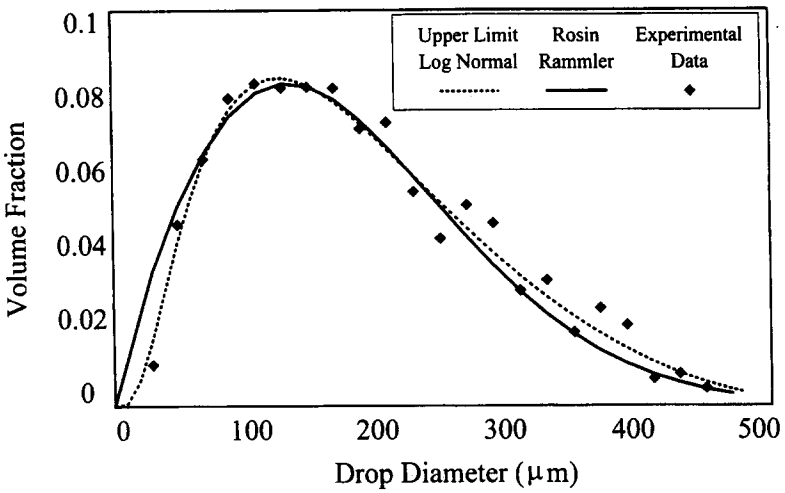

Figure 20. Test of Rosin–Rammler and upper limit log normal distributions against data of Hay *et al.* (1996).

The above distribution functions are illustrated and their ability to fit experimental data tested in figure 20, which shows the fit of data taken by Hay *et al.* (1996) to Rosin–Rammler and ULLN equations. Both equations fit well in the middle of the distribution, with the ULLN giving an overall better fit. However, there is a great deal of scatter at larger sizes. Sauter mean diameters calculated from the fitted Rosin–Rammler equation were 30% lower than those from the raw data. A similar trend has been found for size information obtained from laser diffraction measurements (Azzopardi and Zaidi 1997).

In some cases we might require the maximum size present, a facet covered by a recent review by Azzopardi and Hewitt (1998). Maximum drop sizes could be obtained from the experimental data. However, there is no guarantee that the maximum size observed is the true maximum. Indeed, recent work by Azzopardi and Hibberd (1994) has shown that the ratio of maximum to Sauter mean diameters has a strong dependence on the size of the sample studied, i.e. the number of drops. Figure 21 shows the trend. This implies that the measured maximum drop size will be larger if a greater number of drops is sampled. Azzopardi and Hibberd (1994) have used statistical analysis to show that there can be such a relationship and that it is predictable (figure 22).

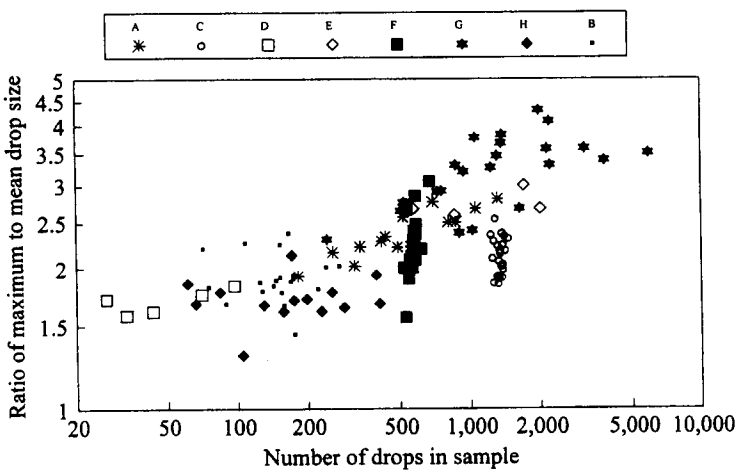

Figure 21. Effect of sample size on the ratio of maximum observed drop size to Sauter mean diameter. (Reproduced from Proc. 6th Int. Conf. on Liquid Atomization and Spray Systems, Azzopardi and Hibberd, "Determination of maximum drop sizes in annular gas/liquid flow", pp. 962–969, Copyright (1994), with kind permission of Begell House Inc, New York, USA.)

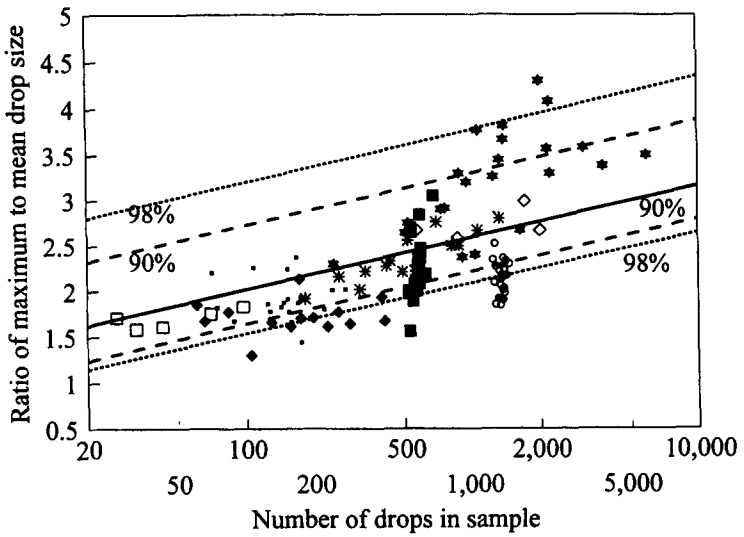

Figure 22. Predicted maximum drop size vs sample size; comparison with experimental data, $\gamma = 1.0$. (Reproduced from Proc. 6th Int. Conf. on Liquid Atomization and Spray Systems, Azzopardi and Hibberd, "Determination of maximum drop sizes in annular gas/liquid flow", pp. 962–969, Copyright (1994), with kind permission of Begell House Inc, New York, USA.)

4.2. *Methods of measurement*

A large number of different techniques have been suggested for the measurement of drop sizes. These have been reviewed by Azzopardi (1979) and Tayali and Bates (1990). Azzopardi concluded that optical techniques were the most suited for the study of annular flow.

Tatterson *et al.* (1977) used charge removal from an insulated probe to determine drop size. They carefully calibrated their equipment and found that the charge removed by a drop was proportional to the square of the drop diameter. The magnitudes of individual charge losses were measured and sorted into a number of discrete bands which could be converted into a drop size distribution.

A needle bridging method was developed and used by Wicks and Dukler (1966). Their equipment consisted of two needles in line with each other with their tips a short distance apart. These are connected in a circuit with a resistance and a battery. When a drop bridges the two needles and completes the circuit a pulse goes through the resistance and is monitored. A pulse indicates that the drop causing the bridge is larger than the gap. The experiment is started with the gap at a large setting, the setting is then reduced progressively and mean count data obtained for each setting. This provides a set of data which could be reduced to the drop size distribution. Wicks and Dukler presented a reduction procedure but McVean and Wallis (1969) have pointed out an error in the method which invalidated their data.

Ueda (1979), Ueda *et al.* (1978) and Okada *et al.* (1995) have captured samples of drops on slides covered with magnesium oxide or viscous oil. They subsequently analysed them under a microscope. Okada *et al.* (1994) describe a number of tests carried out to prove the technique and provide arguments against the importance of a number of possible errors.

Photography has been used by Hewitt (1962), Cousins and Hewitt (1968), Pogson *et al.* (1970), Andreussi *et al.* (1978), Linstead *et al.* (1978) and Hay *et al.* (1996). In all cases drop sizes were determined from enlarged prints. Discrimination was used to include only those drops within a narrow plane. Hay *et al.* (1996) used a sheet of light to illuminate the drop field. The thickness of this sheet was narrower than the depth of focus of the camera and so all drops were in focus.

Azzopardi *et al.* (1978), Azzopardi *et al.* (1980), Azzopardi *et al.* (1983), Azzopardi *et al.* (1991), Gibbons *et al.* (1983), Gibbons (1985), Teixeira *et al.* (1988), Jepson *et al.* (1989), Jepson *et al.* (1990), Jepson (1992), Ribeiro *et al.* (1995), Azzopardi *et al.* (1996) and Azzopardi and Zaidi (1997) have used a diffraction technique. The intensity of scattered light depends on the angle between the incident and observed beams. This angular variation can be calculated. For

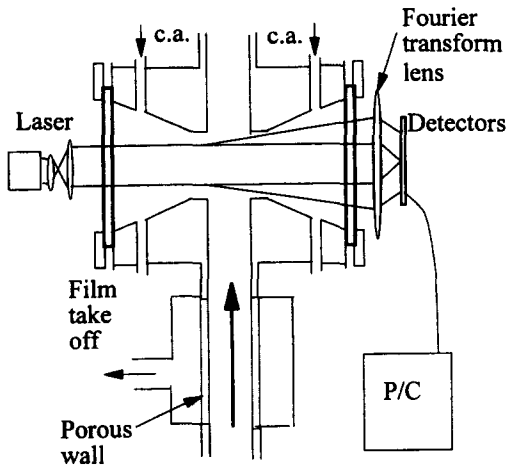

Figure 23. Schematic of Malvern instrument for diffraction based drop size measurement. (Based on figure from Experiments in Fluids, Vol. 3, Azzopardi, "Drop sizes in annular two-phase flow", pp. 53–59, Copyright (1991), with kind permission of Springer-Verlag GmbH & Co. KG, Heidelberg, Germany.)

the size range of interest in annular flow, the intensity of scattered light at a fixed angle is proportional to the drop size squared and can be used to determine drop sizes. However, the constant of proportionality depends on the intensity of the incident light and the obscuration of light by any windows. A more powerful approach is to use the light scattered from an ensemble of particles, particularly light scattered at small forward angles where, for drop sizes of interest to this study, it is dominated by diffraction. This angular variation of scattered light is captured on a set of annular detectors. The areas of these detectors increase with radius. This is an advantage as the range of energies measured is less wide than the corresponding intensity variation. Normally, the drop size distribution would be obtained directly from the energy distribution. However, there are mathematical complications. Instead a size distribution was assumed and used to calculate an energy distribution. The values of the parameters describing the size distribution were adjusted until the best fit between measured and calculated energy was achieved. Swithenbank *et al.* (1976) suggested describing the weight distribution by the Rosin–Rammler distribution, [8]. The characterizing parameters $\bar{X}$, N were then optimized to give the best agreement between the calculated and measured energies. Subsequently the technique has been extended to handle other distribution functions or a 15-parameter model independent algorithm. Instruments based on this technique are marketed by a number of companies. Those most commonly used in annular flow work are from Malvern Instruments Ltd. These use a detector system consisting of 30 annular rings. The arrangement is shown in figure 23. Light from a small He/Ne laser is passed through a beam expander to create a beam of ~8 mm diameter. Beyond the spray and in line with this beam is positioned a Fourier transform lens with the detector at its focal plane. This lens ensures that light scattered from drops at an angle will strike the detector at a fixed radius irrespective of the position of the drop. The focal length of the lens also determines the range of drop sizes that can be analysed. The signal from the detector is sampled by a computer which also performs the analysis described above. Each of the 30 detectors is sampled many times so as to obtain a result from a sufficiently large data-set.

Tests of the diffraction based instruments as produced by Malvern Instruments Ltd (Hammond, 1980, "standard" distributions of polystyrene spheres; and Azzopardi, 1984, photography and sedimentation of suspended glass beads), show good agreement in terms of the Sauter mean diameter (figure 24), however, examination of the distributions shows that for some cases there is good agreement throughout the distribution but in others there are noticeable differences. These differences are not necessarily an indication of inaccuracy in the diffraction instrument but could be due to difficulties in the sampling/photography technique. More reproducible tests are possible using a reticle (Hirleman *et al.* 1984), which consists of an artificial "aerosol" made up of an array of chrome thin-film circles on a transparent glass substrate.

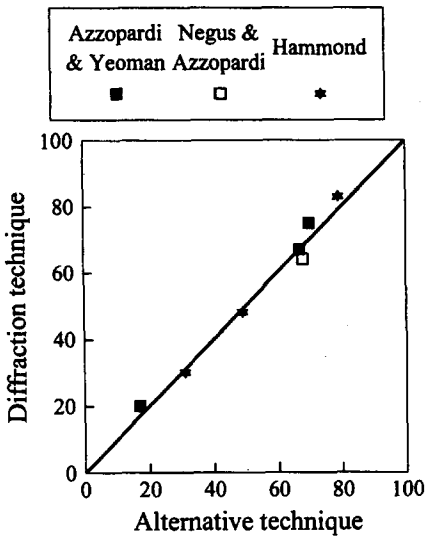

Figure 24. Testing of diffraction based drop sizing instruments, Sauter mean diameters (Azzopardi 1984).

A version containing 13 252 circles whose sizes corresponded to a Rosin–Rammler distribution with parameters $\bar{X} = 50$ and $N = 2.0$ (ref no. 69) was used by Azzopardi (1992) and very good agreement was obtained (figure 25). Hirleman *et al.* used the reticle to check the performance of a Malvern 2200 model. Hirleman and Dodge (1985) found that Malvern Instruments measured this accurately if correction factors were applied to each element of the detector as suggested by Dodge (1984) a procedure now provided routinely by the suppliers. A limitation of the instrument is that light scattered by one drop can be further scattered by others, resulting in errors at sufficiently large concentrations (Azzopardi 1984). A number of workers have put forward methods to correct for multiple diffraction (Felton *et al.* 1985) for those cases where the distribution information was provided in the form of a two parameter equation such as Rosin–Rammler, normal or log–normal (Hamidi and Swithenbank 1986), a method which was not linked to specific distribution equations (Cao *et al.* 1991 and Hirleman 1989).

A technique for the simultaneous measurement of drop size and velocity was developed by Semiat and Dukler (1981) and applied to annular flow by Lopes and Dukler (1985) and in modified form by Fore and Dukler (1995a). An interference pattern is created in the cross section of a laser beam by passing it through a transparent Ronchi diffraction grating. This pattern takes the form of a series of light and dark fringes with the same spacing as the grating. A drop passing through the beam scatters light which is collected by a detector mounted at 45° above the beam. The detected signal contains temporal oscillations from whose frequency the drop velocity, v, can be determined. A second detector picked up the unscattered light. A drop passing through the beam casts a shadow whose residence time, T, can be detected. From these parameters the drop size is obtained via $D = Tv - M$, where M is the size of the detector. Obviously, the size of the detector governs the lower limit of size detected. Lopes and Dukler (1985) had a limit of 100 μm. Fore and Dukler (1995a) extended the technique down to 10 μm by expanding the laser beam after it had passed through the test section but before the detector.

An alternative technique involving residence time was employed by Tayali *et al.* (1990) They used a conventional laser Doppler arrangement in which two laser beams were crossed to product a probe volume consisting of light and dark fringes. Photodiodes monitored the undeviated beams and a photomultiplier placed between the photodiodes collected the light scattered. When either beam is deflected by a drop, then a loss of signal is experienced by the photodiodes and the period of obscuration provides the drop transit time. The velocity is determined from the oscillating scattered light signal. The signals from both photodiodes were compared in an analogue processor to identify the degree of coincidence and so only signals corresponding to

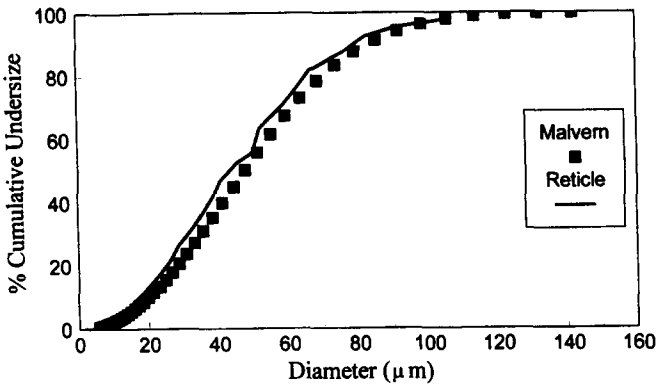

Figure 25. Goodness of fit of drop size distribution to that on reticle of Hirleman *et al.* (1984).

diameters were counted. However, because of the finite size of the probe volume, only larger drops could be handled and the instrument had a range of 75–1500 μm.

Simultaneous measurements of drop size and velocity were made by Azzopardi and Teixeira (1994) using a phase Doppler anemometry technique. The beam of a 15 mW He/Ne laser was split into two equal intensity beams 15 mm apart. They were focused by a 310 mm focal length lens (crossing angle 2.77°) and the scattered light collected at three positions (at an offset of approximately 30° from the forward direction). This arrangement produces an instrument with a wide dynamic range and from whose signals sphericity can be determined. The signals are filtered and processed from which the frequency (and hence velocity) and phase lag (size) can be determined. A microcomputer calculates the velocity and size and sorts and stores the data. For the present optical geometry the size range is 30–650 μm. Because of the Gaussian distribution of intensity of the laser beams, the effective probe volume will be larger for bigger drops at a given trigger level. A correction has been made for this.

4.3. *Sources of errors*

Measured drop size distributions are subject to error from several sources. There are those which are associated with the specific measurement methods and which have been discussed in connection with each method. However, here we consider those errors of a statistical nature which arise from counting and measuring a finite sample of drops and so determining the drop size distribution or mean diameters. Because of the complexities involved it should not be surprising that the minimum number of drops will depend on the type of distribution considered. For number distribution, the corresponding mean, D_{10}, demands that all classes are equally weighted so that standard statistical approaches can be used. For higher order distributions such as $v(D)$, the weighting by D^3 of each drop class puts more emphasis on the larger drop sizes. In considering this problem, we must remember that one 1000 μm drop contains as much liquid as 1000 of 100 μm. The upper tail of the distribution is thus very important and it is necessary to measure a sufficiently large number of drops in the largest size class. For the Sauter mean diameter, D_{32}, Bowen and Davies (1951) have estimated (within the 95% confidence limits) that the accuracies in table 5 require the sample sizes shown.

A recurring problem with methods which count individual drops (photography, laser anemometry, capture on oil covered slides) is how to allow correctly for the effect of large drops. Hay *et al.* (1996) argue that to obtain accurate mass distributions, either a very large number of drops need to be measured or a method needs to be developed to improve the statistical representation of large drops. They allowed for this by measuring all small drops over a small volume and large drops over a larger volume. The two distributions are then merged via appropriate normalization. However, as seen in figure 20, their data, particularly at the higher size end shows a very irregular profile, in spite of the care taken by the researchers and the fact that they measured several thousand drops. Okada *et al.* (1995) have noted that a single large drop can have very significant influence on the Sauter mean diameter. Their work shows that the omission of a small number of large drops can cause large differences in Sauter mean diameter,

Table 5.

Sample size	500	1400	5500	35 000
Accuracy	17%	10%	5%	2%

although it has a much smaller effect on the arithmetic mean. A similar effect is apparent from reanalysis of the data of Cousins and Hewitt (1968).

Several of the measurement techniques described above are based on the assumption of spherical drops. Larger drops have been observed to be non-spherical and could thus be counted at a size other that the correct equivalent diameter.

A problem common to all applications of optical techniques to annular flow is overcoming the effect of the curved tube wall and the wavy interface of the film. Hewitt (1962), Pogson *et al.* (1970) and Andreussi *et al.* (1978) removed the liquid film and photographed the drops in the ensuing jet. In contrast, Linstead *et al.* (1978) used a window placed at the end of the tube to obtain optical access. Tayali *et al.* (1990) and Hay *et al.* (1996), as well as the workers who used diffraction, stripped off the film through a porous wall section or a slit. They then placed flat windows at the end of side arms located just downstream. Jets of compressed gas kept these windows free of drops. A typical arrangement is shown in figure 23. Teixeira (1988) has shown that the amount of air sucked off with the film and the gas pressure used for purging have no effect on the measured drop sizes, provided these variables are kept below experimentally determined values. Gibbons *et al.* (1983), Lopes and Dukler (1985), Azzopardi and Teixeira (1994) and Fore and Dukler (1995a) used tubes or glass rods which passed through the tube wall and the film. Where necessary windows were placed on the outer ends of these tubes. Gibbons *et al.* (1983) used both tubes and film suck-off techniques and found no differences in the results obtained for the same flow conditions.

4.4. *Available data*

Table 6 lists published papers which give data of drop sizes in annular two phase flow. Data is for air–water unless noted. As noted above doubts have been expressed about the techniques of Wicks and Dukler (1966) and Tatterson *et al.* (1977). The photographic technique used by Linstead *et al.* (1978) probably did not have the resolution to pick up the large number of drops at smaller sizes. Similarly, the laser Doppler techniques used by Lopes and Dukler (1985) and Tayali *et al.* (1990) have lower limits of 100 μm and 75 μm respectively and, therefore, miss a significant proportion of the drops. In addition, the data sets of Hewitt (1962), Pogson *et al.* (1970), Ueda *et al.* (1978) and Ueda (1979) have sample sizes which according to Bowen and Davies (1951) would result in large uncertainty, table 5. Thus those data should only be used with great care.

Before considering the effect of various parameters on drop size, it is important to check the comparability of data from different workers and different techniques. Azzopardi and Teixeira (1994) have gathered drop size distribution information under identical conditions using the diffraction and phase Doppler techniques. When the raw data from each technique are compared, there is a significant difference between them. In addition, Sauter mean diameters obtained from the raw phase Doppler data showed surprisingly little effect of gas and liquid flow rates. A number of reasons have been identified for the differences. Teixeira (1988) suggested that the major reason to be that the phase Doppler system is triggered by the amplitude of the signal and, due to the Gaussian profile of the light intensity inside the probe volume, larger drops are more likely to be measured than small ones. He argued that, at the larger sizes, the drop size distribution should, but does not, approach zero smoothly and possibly the relative proportion of large to small drops is unrealistic. Teixeira used a simple truncation technique to compensate for this. In a distribution plot, where the drop frequency first dropped to zero, drops larger than this were discounted. An alternative technique based on an effective probe area correction was also applied and gave similar results. Once this, and allowance for radial variations and for drop size–velocity relations was made, good agreement was obtained in drop size distribution between both techniques. Similar agreement between these two measurement methods has been observed by Brazier *et al.* (1988), who studied the drops formed by a spray nozzle. However, it

Table 6. Sources of data for drop size in annular flow

Orientation	Source	Pipe diameter (m)	Pressure (bar)	Superficial velocity (m/s)		Distribution function	Notes
				Gas	Liquid		
U	Hewitt (1962)	0.032	1	26–66	0.032–0.238	—	
D	Wicks and Dukler (1966)[a]	0.152 × 0.019	1	25–86	0.022–0.175	—	
U	Cousins and Hewitt (1968)	0.0095	2.2	27–47	0.06–0.39	—	
U	Pogson *et al.* (1970)[b]	0.034	1	70	0.014–0.043	NT	Steam/water
H	Tatterson *et al.* (1977)[a]	0.305 × 0.025	1	26–60	0.044–0.018	ULLN	
D	Andreussi *et al.* (1978)	0.024	1	26–65	0.036–0.29	ULLN	
U	Azzopardi *et al.* (1978)	0.032	1.5	24–44	0.016–0.095	RR	
U	Linstead *et al.* (1978)[c]	0.032	1.1	7–22	0.001–0.09		
U	Ueda *et al.* (1978)[b]	0.01	~3	10–27	0.02–0.114	Γ	R113
U	Ueda (1979)[b]	0.01 0.03	1	43–85		Γ	Also low surface tension and higher viscosity liquid
U	Azzopardi *et al.* (1980)	0.032	1.5	23–42	0.016–0.16	RR	
U	Azzopardi *et al.* (1983)	0.125	1	30–43	0.008–0.026	RR	
U	Gibbons (1985)	0.032	1.5	31–44	0.048	RR	Aq. Glycerol Soln $\acute{\eta}_l = 0.001$–0.022
U	Lopes and Dukler (1985)[c]	0.05	~1	14–25	0.034–0.121	ULLN	
U	Teixeira *et al.* (1988)	0.032	1.5	26–50	0.016–0.125	RR	
U	Jepson *et al.* (1989)	0.01	1.5	22-67	0.04-0.14	RR	
		0.01	1.5	44–76	0.04–0.15	RR	Helium/water
U	Jepson *et al.* (1990)	0.01	1.5	8–24	0.03–0.122	RR	Air/1,1,1 trichloroethane
U	Tayali *et al.* (1990)[c]	0.032	1.6	10–32	0.013–0.032		
U	Azzopardi *et al.* (1991)	0.02	1.5	30–59	0.041–0.124	RR	
U	Jepson (1992)	0.01	1.5	28–42	0.04–0.14	RR	CF_4/water
U	Azzopardi and Teixeira (1994)	0.032	1.5	13.6–31	0.016–0.048		
U	Fore and Dukler (1995a)	0.05	1–1.2	17–33	0.015–0.06	ULLN	
			1–1.2	16–32	0.017–0.067	ULLN	Aq. glycerol soln $\acute{\eta}_l = 0.006$ kg/ms
U	Hay *et al.* (1996)	0.042	~1	36	0.022–0.123	ULLN/RR	
U	Okada *et al.* (1995)	0.03	~1	28–47	0.01–0.15		Centre jet injector
H	Ribeiro *et al.* (1995)	0.032	1.3–1.4	25–42	0.03–0.11		
H	Azzopardi *et al.* (1996)	0.065	~1	17–25	0.11–0.16	MI	
V,I,H	Azzopardi and Zaidi (1997)	0.038	1.5	15–30	0.02–0.16	MI	Every 10° between vertical upwards and horizontal
V,I,H	Zaidi and Altunbas (1997)	0.038	1.5	15–30	0.02–0.16		

[a]Unreliable technique. [b]Sample size too small. [c]Technique misses small drops.

is possible that the explanation given above is too simple. Fault might lie in the Rosin–Rammler equation used to fit the distribution in the diffraction technique. An alternative analysis which does not prescribe an equation indicates the presence of more large drops than fitting the Rosin–Rammler equation would permit (figure 26). In fact plotting maximum drop sizes (identified as D_{99}, the size below which 99% of the liquid by mass is contained) shows agreement between the laser Doppler data of Fore and Dukler (1995a) and the diffraction data of Azzopardi and Zaidi (1997), which they analysed with the model independent approach

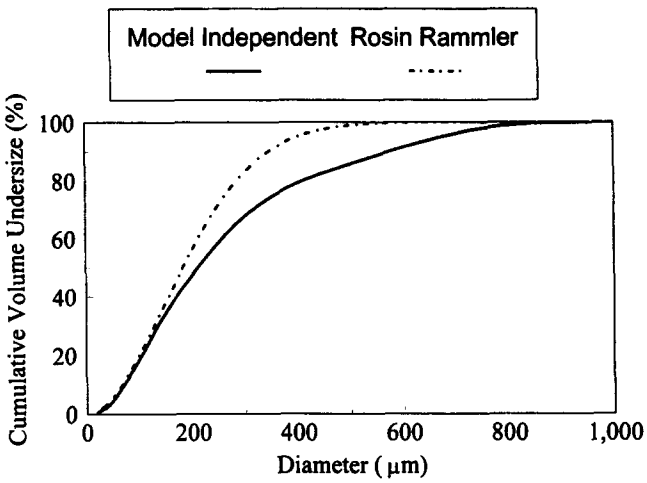

Figure 26. Results from laser diffraction technique analysed using Rosin–Rammler and model independent approaches—pipe diameter = 0.038 m; gas superficial velocity = 33 m/s; pressure = 1.8 bar.

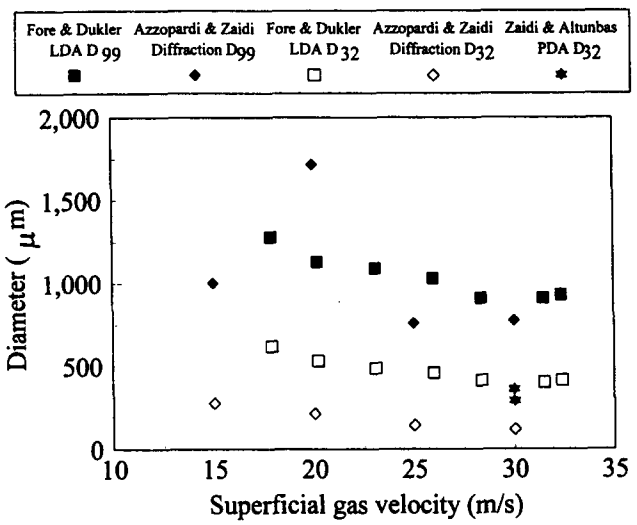

Figure 27. Comparison between maximum and Sauter mean diameters from laser Doppler technique (Fore and Dukler 1995a); laser diffraction technique analysed using model independent approach (Azzopardi and Zaidi 1997), and phase Doppler technique (Zaidi and Altunbas 1997).

(figure 27). In contrast the Sauter mean diameters obtained by Fore and Dukler and Azzopardi and Zaidi vary significantly†. This could be in part due to bias in the laser Doppler technique as discussed above. Another reason could be that in the diffraction experiments measurements were made using a film strip-off section, i.e. a short distance downstream of the last creation of drops. In contrast, Fore and Dukler did not strip off the film but passed the illuminating and scattered light through glass rods and were thus closer to drop creation. Given that large, short-lived drops have been observed, this could explain the difference. Raw phase Doppler data obtained by Zaidi and Altunbas (1997) on the same test section and at similar flow rates to those employed by Azzopardi and Zaidi (1997) gave a Sauter mean diameter closer to those obtained by Fore and Dukler (1995a). This suggests that all previous diffraction data originally analysed using the Rosin–Rammler approach should be reanalysed using the model independent approach. However, as the majority of data discussed below were taken using diffraction/Rosin–Rammler, it is possible to use it to identify parametric trends.

†The Sauter mean diameters obtained from the model independent analysis differ by only 30% from that obtained from the Rosin–Rammler analysis. This ratio is similar to that obtained by Hay *et al.* (1996) from photographic data.

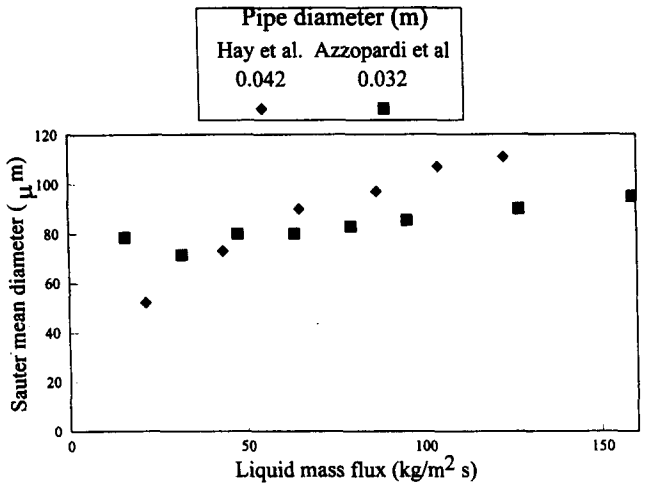

Figure 28. Comparison of drop size measurements from Hay *et al.* (1996) and Azzopardi *et al.* (1980).

The data of Hay *et al.* (1996) have been compared with those of Azzopardi *et al.* (1980). For the Hay *et al.* data the Sauter mean diameters were determined from the fitted Rosin–Rammler parameters. This approach was used as the other data had been obtained in the same way. Figure 28 shows reasonable agreement between the sources except at the lowest liquid flow rates where most of the data show increasing drop size with decreasing liquid flow rate whilst those of Hay *et al.* (1996) show a decrease. The data sets are taken from different pipe diameters, but as will be discussed below this parameter should not have much effect.

The effect of tube orientation on drop size can be examined by considering the data of Andreussi *et al.* (1978), Azzopardi *et al.* (1980), Ribeiro *et al.* (1995), Azzopardi and Sudlow (1996) and Azzopardi and Zaidi (1997). Azzopardi (1985) has shown that there is good correspondence between the downflow data of Andreussi *et al.* (1978) and that of Azzopardi *et al.* (1980) for upflow. However, the gas velocities were significantly high so that the differences should be minimal. Azzopardi and Zaidi measured drop sizes for a range of gas and liquid flow rates at every 10° of inclination between vertical upwards and the horizontal. Figure 29 shows that, although there not much of an effect of angle between vertical (0°) and about 40°, the drop sizes appear to change to a higher value beyond this point. Hitherto no definite expla-

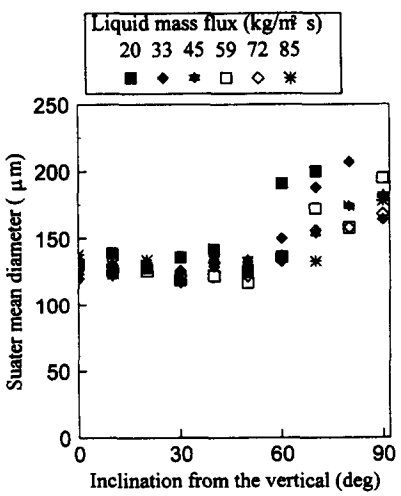

Figure 29. Effect of inclination on drop size—pipe diameter = 38 mm; pressure = 1.5 bar. (Reproduced from 4th World Congress on Experimental Heat Transfer, Fluid Mechanics and Thermodynamics, Vol. 2, Azzopardi and Zaidi, "The effect of inclination on drop sizes in annular two-phase flow", pp. 1167–1174, Copyright (1997), with kind permission of Edizioni ETS s.r.l., Pisa.)

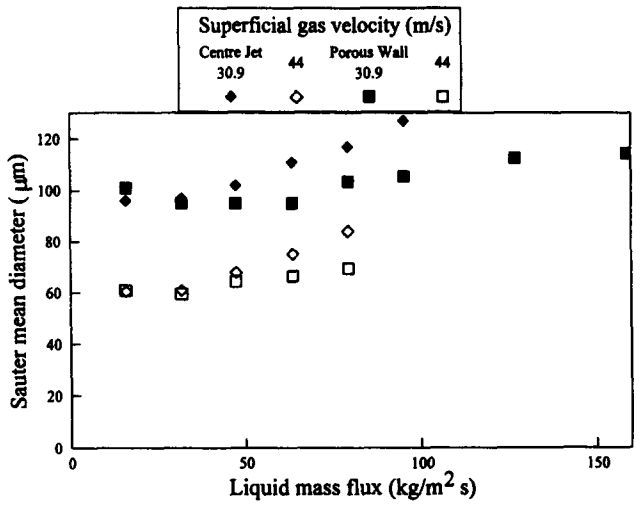

Figure 30. Effect of method for liquid injection on drop size. (Based on figures from Experiments in Fluids, Vol. 3, Azzopardi, "Drop sizes in annular two-phase flow", pp. 53–59, Copyright (1991), with kind permission of Springer-Verlag GmbH & Co. KG, Heidelberg, Germany.)

nation has been found for this, but one possible cause is the thicker films found at the lower part of the pipe in the more shallowly inclined cases. In contrast to this result, comparison of the vertical upflow data of Azzopardi *et al.* and the horizontal data of Ribeiro *et al.* shows that drop sizes from vertical flow are larger than the equivalent value from the horizontal tube experiment, although this difference diminishes as the gas velocity increases. The measurements were made at slightly different conditions but it is not known which of these is the most important.

The effect of method of injection was tested by Azzopardi *et al.* (1980). Figure 30 shows that the data from a centre jet injector gives slightly larger sizes than when the liquid is introduced through a section of porous wall.

The effect of gas flow rate is illustrated in figure 31. Similar trends are reported by most workers. Drop sizes decrease with increasing gas velocity. This is consistent with the concept that the process is shear driven and the higher the gas velocity the greater the shear and the smaller the drops. Most workers find that drop size depends on gas velocity to a power of about −1.1. A major exception to this has been suggested by Ueda (1979) who identified the

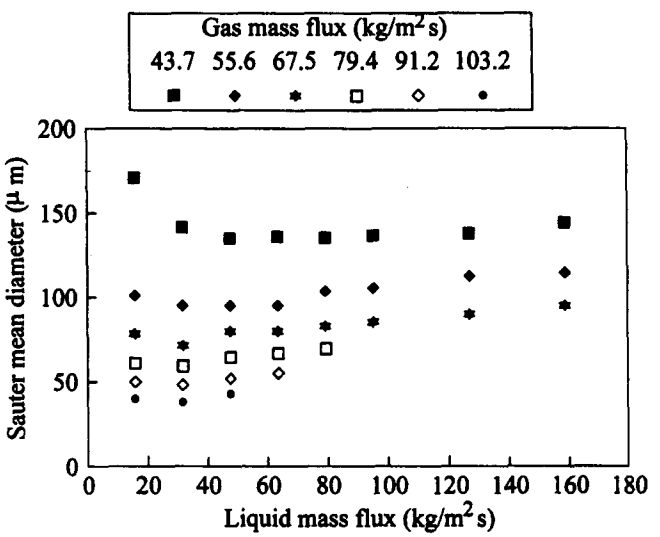

Figure 31. Example of the effect of gas and liquid flow rates on drop size. (Based on figure from Experiments in Fluids, Vol. 3, Azzopardi, "Drop sizes in annular two-phase flow", pp. 53–59, Copyright (1991), with kind permission of Springer-Verlag GmbH & Co. KG, Heidelberg, Germany.)

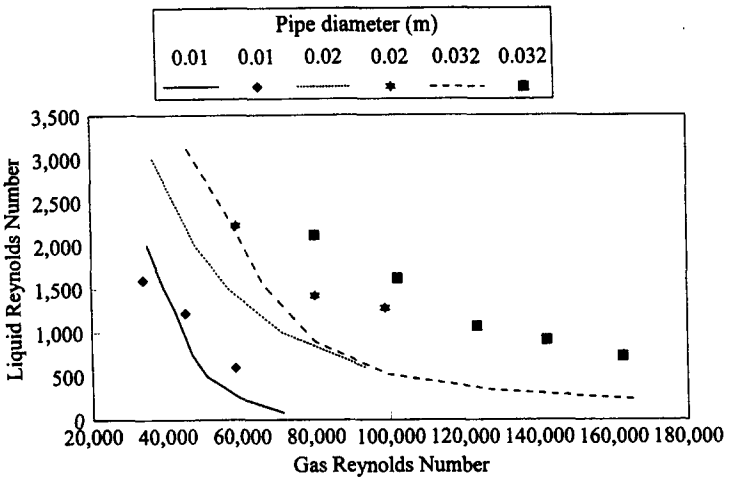

Figure 32. Dimensionless map showing boundary between entrainment mechanisms.

power as –0.3. Two reasons can be proposed for this difference. Firstly, it was noted above that the data of Ueda was based on small samples of drops with a consequent large uncertainty in the mean diameter. Secondly, Ueda give no information about the liquid flow rate. It is possible that, if the effect of liquid flow rate is correctly allowed for, the data would show a power relation with gas velocity nearer to that reported by most other workers.

The effect of liquid flow rate is shown in figure 31. Increasing the liquid flow rate results in first a decrease and then an increase in drop size. Azzopardi (1983) suggested that the two different slopes are due to the dominance of each of the two mechanisms discussed above and indicated that there appeared to be a similarity between these mechanisms and those occurring when drops break up in gas streams. Transitions in the latter are known to be governed by a Weber number based on the original drop diameter. Azzopardi suggested that a similar approach might apply for annular flow. Here the Weber number was based on the wave height, We_w. The transition was taken to correspond to the minimum in the drop size–liquid flow rate data. More data has been gathered by Jepson (1992). This has all been replotted as Reynolds numbers of the phases (figure 32). The lines are the locus of $We_w = 25$. Although there is not perfect agreement between the data for each pipe diameter, both the curves and the symbols representing the minima show the same trends. The non-dimensional groups chosen bring the data closer together than when considered as mass fluxes. However, at this stage it must be concluded that, although the approach looks promising, there is still a need for more data and analysis.

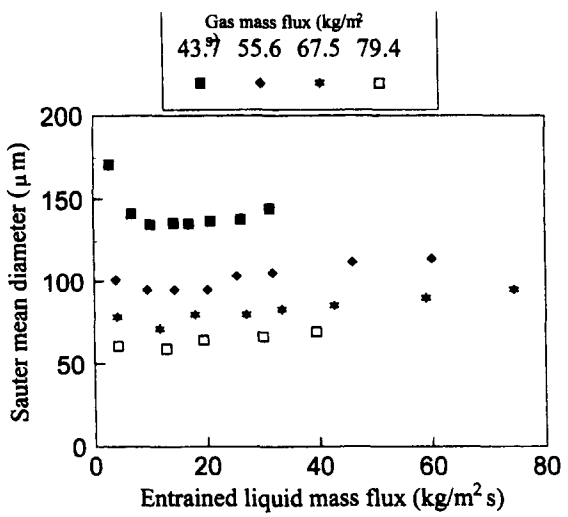

Figure 33. Plot of drop size against entrained liquid mass flux.

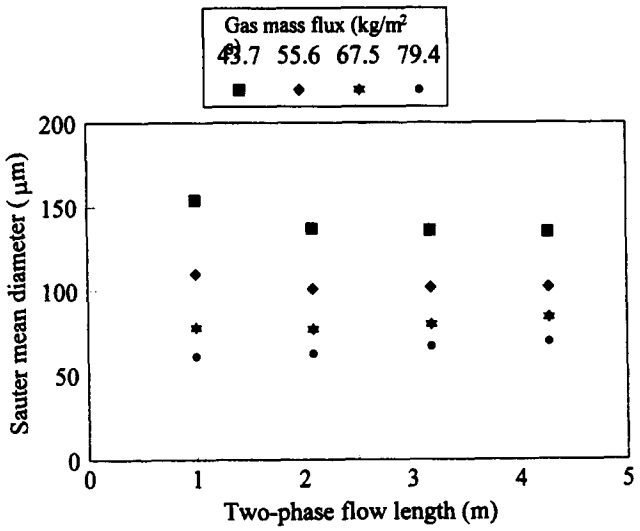

Figure 34. Drop size measurements—effect of two-phase flow length. (Based on figure from Experiments in Fluids, Vol. 3, Azzopardi, "Drop sizes in annular two-phase flow", pp. 53–59, Copyright (1991), with kind permission of Springer-Verlag GmbH & Co. KG, Heidelberg, Germany.)

In figure 30, the majority of the data show an increase in drop size with liquid flow rate. When the drop sizes were plotted against entrained liquid flow rate, the data lie on straight lines, as seen in figure 33. Further evidence that the drop size depends on the entrained liquid flow rate is given by Azzopardi (1985) who reported three series of measurements. The first (A) were made using a porous wall injector for the liquid. Gas and liquid flow rates were varied and data were taken at a fixed length from the mixer. A second series (B) used the porus wall injector and measurements were taken at a number of distances from the injector. The third series (C) was identical to the first except that the liquid was injected through an axial pipe in the centre of the test section. Examples from series A and C were shown in figure 30. The effect of varying the two-phase flow length are illustrated on figure 34 and indicate a small but significant variation with two-phase flow length. When this data and that from the series A experiments (where the liquid flow rate was varied) were plotted against entrained liquid mass flux, the two data sets had the same trend. In contrast, when the data are plotted against liquid film mass flux, the data show opposite trends. Azzopardi (1985), therefore, suggested that the drop size depends linearly on entrained liquid mass flux or drop concentration. This is probably due to

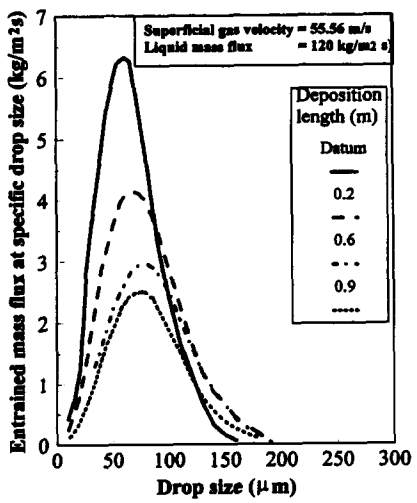

Figure 35. Quantity of the total liquid entrainment at a specific drop size (air/water) (Jepson *et al.* 1989).

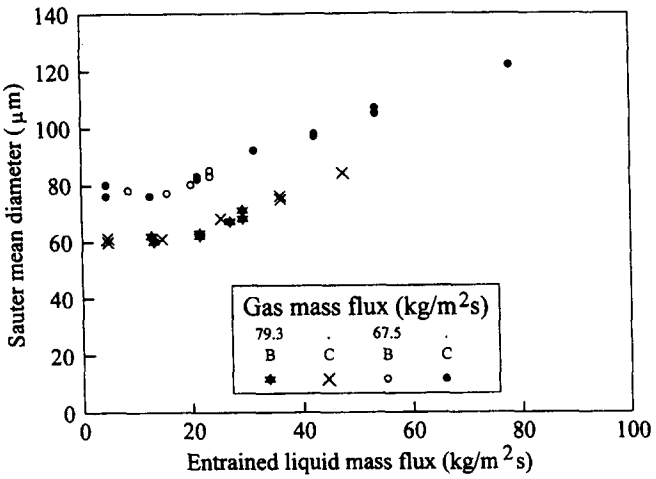

Figure 36. Drop size plotted against average entrained liquid mass flux—series B and C data. (Based on figure from Experiments in Fluids, Vol. 3, Azzopardi, "Drop sizes in annular two-phase flow", pp. 53–59, Copyright (1991), with kind permission of Springer-Verlag GmbH & Co. KG, Heidelberg, Germany.)

coalescence, larger drops removing smaller drops from the flow and thus increasing in size. This view is now generally accepted (Fore and Dukler 1995a; Hay *et al.*, 1996). However, for Fore and Dukler's data the slope of the drop size–concentration plot is 15 times the equivalent slopes for the data of Azzopardi (1985) and Hay *et al.* (1996). More detailed proof of the occurrence of coalescence is given by Jepson *et al.* (1989). They made measurements at a number of distances downstream of where the film had been removed from a well-developed annular flow. The results were plotted as drop size distributions whose integral values corresponded to the entrained liquid mass flux at the position of measurement. As seen in figure 35, there are more larger drops at the intermediate position than at the datum. As the film had been stripped off, the extra, larger drops could not have been produced by the entrainment process. They must be the product of coalescence. It is noted that the process occurring here is similar to that by which wet scrubbers work—larger drops collecting smaller ones and therefore growing. In addition, it should not be surprising that coalescence is not visible in the many high speed films made of annular flow, as in those films the larger drops were the limit of resolution and the smaller, collected drops would not have been visible.

The differences due to the methods of injection of the liquid (series A and C discussed above) can be explained via concentration–length relationships. In the series A experiments the concen-

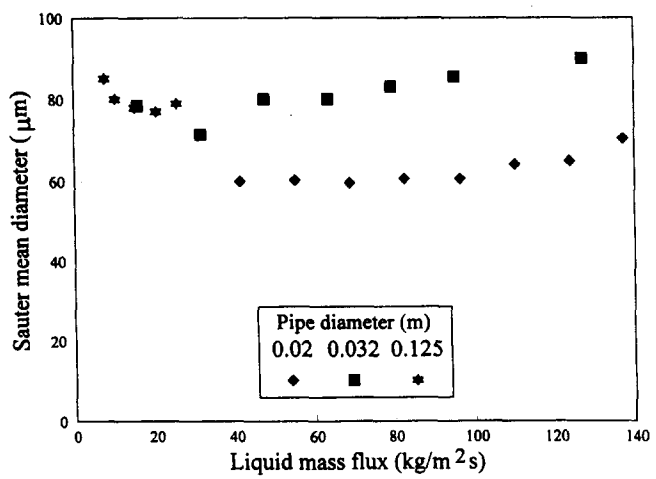

Figure 37. Effect of pipe diameter on drop size.

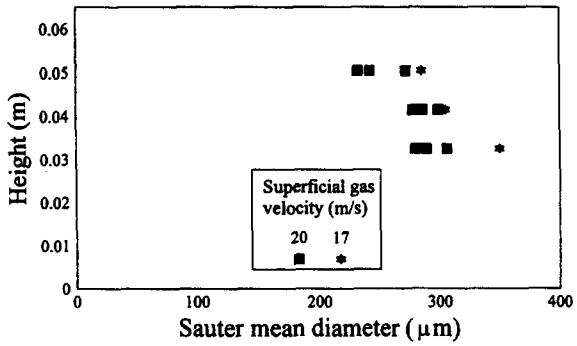

Figure 38. Variation of drop size with vertical position in a horizontal tube (Azzopardi *et al.* 1996).

tration increases from zero at the inlet. Therefore, the average value over the length of the tube, the average value that drops from various sources will encounter, will be below that at the measuring station. In contrast, in the series C experiments, where it was introduced through a centre jet, the data of Gill *et al.* (1968) and Brown *et al.* (1975) indicate that the concentration drops rapidly from its initial high value, when all the liquid is entrained, to a fairly steady value at which it remains for the greater part of the tube. To a reasonable approximation, the concentration can be taken as that at the measurement position. Consequently, when the data is replotted as drop size against mean entrained liquid mass flux, the series C data will be relatively unchanged, whereas the series A and B data would appear at lower liquid mass fluxes, thus placing it closer to the line of the series C data. In those cases where entrained liquid mass flux data is available, a more quantitative check yields good agreement (figure 36).

The influence of pipe diameter for vertical upflow can be seen in figure 37. Here all sets were taken at approximately the same gas velocity. No data was available at this velocity for the 0.01 m diameter pipe. However, interpolated values would lie below those for the 0.02 m diameter pipe. Thus it can be seen that up to about 0.03 m there is a noticeable diameter effect but that above this value the effect is negligible. The effect of pipe diameter in horizontal flow can be examined via the data of Ribeiro *et al.* (1995) who used a 0.032 m diameter tube and made measurements which were an integral over an 18 mm vertical strip and Azzopardi *et al.* (1996) used a 0.065 m diameter pipe and measured along the horizontal diameter and along chords 9 and 18 mm above this. In all cases the beam was 18 mm in diameter. Figure 38 shows that the drop size increases the lower in the pipe the measurement was made. In addition, data from various pipe diameters show the effect of gas velocity on the drop size (figure 39). The data from

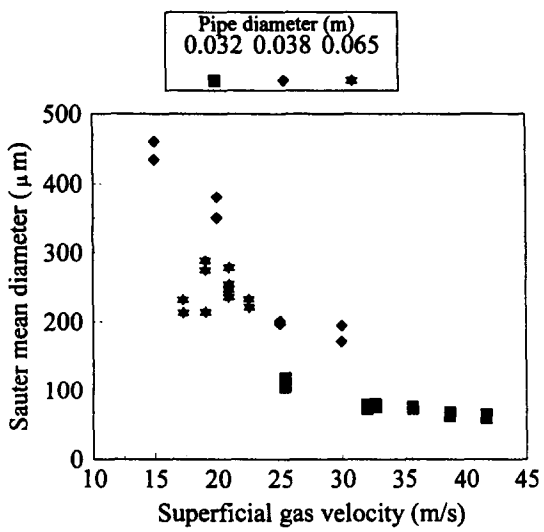

Figure 39. Effect of gas velocity on drop size—horizontal annular flow.

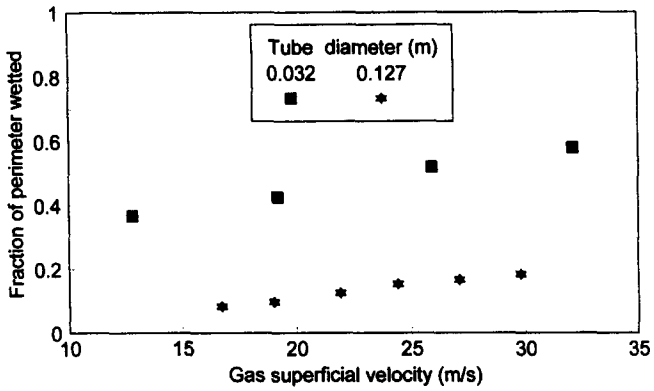

Figure 40. Effect of tube diameter on fraction of wall wetted (Rea and Azzopardi 1996).

the larger diameter pipe appear to indicate drop sizes greater than those extrapolated from the smaller tube data. This is probably due to the liquid being gathered in a thicker film at the bottom for the larger diameter pipe. Support for this is seen in figure 40 where the effect of pipe diameter on the fraction of wall wetted in stratified flow has been plotted for a number of pipe diameters. For the same superficial velocities, the liquid wetted portion decreases with increasing pipe diameter.

The effect of pressure, or more correctly gas density, has been examined by Gibbons (1985) and Jepson (1992). The former working with an air–water system, varied the pressure to produce gas densities in the range 1.2–2.3 kg/m^3 and observed an increase in drop size with gas density. However, the experiments were carried out at constant mass flux so that it is not clear whether the increase was due to the change in density or the consequent decrease in gas velocity. Jepson achieved gas densities in the range 0.27–5.0 kg/m^3 by using a number of different gases. In all cases the liquid was water. At a gas velocity of 33 m/s the drop size decreased slightly when the gas density was increased from 1.8 to 5.0 kg/m^3 but at 44 m/s drop size data showed a minimum as gas density went from 0.27 to 5.0 kg/m^3. Jepson has questioned whether these effect are entirely due to changes in gas density and suggests that there might also be an effect of the different mechanisms discussed above.

The effect of liquid viscosity on drop size has been studied by Ueda (1979), Gibbons (1985) and Fore and Dukler (1995a). In all cases the viscosity was varied by adding different proportions of glycerol to water. Ueda increased the viscosity to eight times that of water and found very little variation in drop size. Gibbons used viscosities up to twenty times that of water and found that the drop size only increased by 25%. Fore and Dukler employed liquids with viscosities of 0.001 and 0.006 kg/ms and found a small but noticeable increase in drop size.

Ueda (1979) and Jepson *et al.* (1990) have examined the effect of surface tension. As might be expected lowering surface tension reduces drop size. However, it is not possible to determine a simple parametric effect directly, probably because of the different mechanisms described above.

4.5. *Equations to predict drop size*

Although a number of equations have been proposed to predict the effect of appropriate parameters on drop sizes, they are all semi-empirical. Tatterson *et al.* (1977) based their model on the assumption of Woodmansee and Hanratty (1969) that atomization is governed by a Kelvin–Helmholtz mechanism, i.e. that the destabilizing force is the pressure variation over the wave. In this analysis they followed Taylor (1940) but allowed for a finite depth of liquid. The resulting equation was

$$\frac{D}{\delta} = AWe_m^{0.5} = A\left(\frac{\rho_g u_g^{*2}\delta}{\sigma}\right)^{0.5}. \qquad [15]$$

The gas friction velocity u_g^* is used in the Weber number as Tatterson *et al.* argued that it best represented the effect of the gas flow close to the surface of the atomizing waves. This

equation was optimized against the data of Wicks and Dukler (1966), Cousins and Hewitt (1968) and Tatterson (1975). However, as pointed out above, these data must be considered of doubtful value.

Andreussi *et al.* (1978) developed an empirical two-term equation based on their own data. The first term was inversely proportional to square of the gas superficial velocity whilst the second depended on the square root of the film thickness.

The empirical equation of Ueda (1979) contained a single term and the drop size depended on the gas velocity to the power of −0.34. This is contrast to most other equations which show a power of about −1.0.

An equation based on a model in which the drop size depends on the break up of liquid packages in the gas stream was published by Azzopardi *et al.* (1980). This was based on the earlier work of Sevik and Park (1973) and assumed that break-up occurred when the natural frequency of oscillation of the liquid package was equal to the characteristic frequency of turbulence and resonance occurs. Azzopardi *et al.* added a second term (linear in drop concentration) to account for the effect of liquid flow rate on drop size. They attributed this effect to coalescence between drops. Their equation was

$$\frac{D_{32}}{D_t} = 1.91 \frac{Re_g^{0.1}}{We^{0.6}} \left(\frac{\rho_g}{\rho_l}\right)^{0.6} + 0.4 \frac{\dot{m}_{lE}}{\rho_l u_{gs}}, \qquad [16]$$

where

$$We = \frac{\rho_g u_{gs}^2 D_t}{\sigma}$$

and

$$Re_g = \frac{\rho_g u_{gs} D_t}{\eta_g}$$

Lopes and Dukler (1985) and Kocamustafaogullari *et al.* (1993) followed a similar approach and optimised their equation on their own data. They did not use a second term.

[16] indicates that drop size will depend on the square root of the tube diameter. This is contrary to what is observed in larger diameter tubes. Azzopardi (1985) argued that this was due to curvatures other than that of the tube wall (that due to the wave) being more important. An alternative length scale was proposed ($\lambda_T = \sqrt{[\sigma/\rho_l g]}$). This resulted in

$$\frac{D_{32}}{\lambda_T} = \frac{15.4}{\left(\frac{\rho_l}{\rho_g} We_{\lambda_T}\right)^{0.58}} + 3.5 \frac{\dot{m}_{lE}}{\rho_l u_{gs}} \qquad [17]$$

where $We_{\lambda_T} = (\rho_g u_{gs}^2 \lambda_T)/\sigma$.

More complex versions of [16] and [17] have been produced by Gibbons (1985) and Azzopardi *et al.* (1989), but these corrections were all empirical.

The latest and most complex equation has been produced by Ambrosini *et al.* (1991). This combined the ideas of Tatterson *et al.* (1977) and Azzopardi *et al.* (1980). The effect of coalescence of drops is handled in a manner similar to gas kinetic theory by defining a mean-free-path between collisions

$$\lambda_c = \frac{C}{D^2 N} \qquad [18]$$

where N is the number of drops per unit volume and is given by

$$N = \frac{\dot{m}_{lE}}{\rho_l u_{gs}} \frac{6}{\pi D^3}. \qquad [19]$$

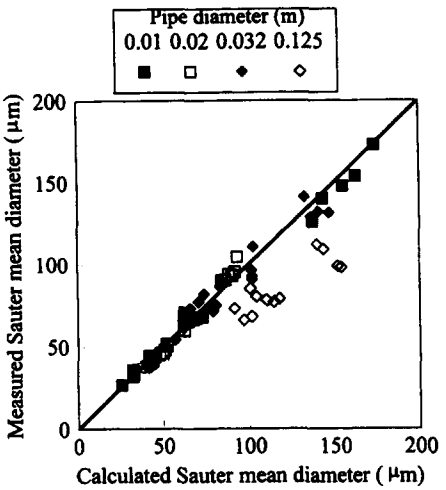

Figure 41. Test of equation of Ambrosini *et al.* (1991)—effect of tube diameter.

The constant C depends on the assumptions made in calculating the drop relative velocity. The probability that a drop has not experienced any collisions after having travelled an overall distance L in the gas can be expressed as

$$P_{nc} = \exp\left(-\frac{L}{\lambda_c}\right). \quad [20]$$

Then it is assumed that the length L scales as the tube diameter and the increase in drop diameter due to coalescence is inversely proportional to P_{nc} to some power. This assumption can be explained using the simplified argument that at each collision the drop increases its volume by a quantity equal to its initial volume. Therefore, after travelling a distance L, the average diameter of a population equal drops is increased by a factor of $(1 + L/M_c)^{0.333}$. $1 + L/M_c$ can approximated by an exponential. The effects suggested by Tatterson *et al.* and Azzopardi *et al.* are combined by a square averaging technique and some manipulation and approximating the square root by an exponential results in

$$\frac{D_{32}}{\delta} = 22\left(\frac{\sigma}{\rho_g f_i u_g^2 \delta}\right)^{0.5}\left(\frac{\rho_g}{\rho_l}\right)^{0.83}\exp\left(0.6\frac{\dot{m}_{lE}}{\rho_l u_g}\frac{D_t}{D_{32}} + \frac{99}{We}\right). \quad [21]$$

Ambrosini *et al.* also provide correlating equations for film thickness, δ, and the interfacial friction factor, f_i.

The above prediction methods have been tested by Jepson (1992) against a bank of data obtained with the diffraction technique. This covered diameters from 0.01 to 0.125 m, gas densities from 0.27 to 5 kg/m^3 and surface tensions of 0.073 and 0.0258 N/m. The exercise showed that the equations of Tatterson *et al.* (1977) and Ueda (1979) both significantly under predicted whilst those of Andreussi *et al.* (1978) and Lopes and Dukler (1985) over predict. The equation of Azzopardi *et al.* (1980) gives good predictions for most data, exceptions are the helium–water data which is under-predicted and the carbon tetrafluoride–water and air–1,1,1 trichloroethane data were slightly under-predicted. The equation of Azzopardi (1985) gives good predictions except for the carbon tetrafluoride–water data, which are over-predicted. There is also significant scatter for the helium–water data. The equation of Gibbons (1985) also performs well, although the effect of gas density is not well handled, helium–water is under-predicted and carbon tetrafluoride over-predicted. The method suggested by Ambrosini *et al.* (1991) gives good prediction for almost all data. Poorest predictions are for the data from the largest tube (0.125 m). Figure 41–43 compare the prediction of the Ambrosini *et al.* correlation with experimental data. The effects of tube diameter, gas density and surface tension are examined. It is noted that the method of Ambrosini *et al.* does not give good predictions of the effect of liquid

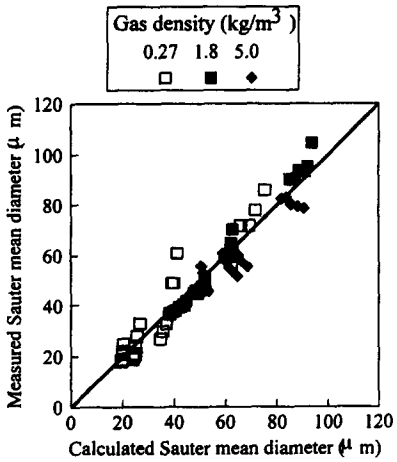

Figure 42. Test of equation of Ambrosini *et al.* (1991)—effect of gas density.

viscosity. This is possibly due to the equations used for film thickness and interfacial shear stress not being so accurate for higher viscosities.

It is illustrative to apply these equations to industrial ranges of parameters. For example, for a low surface tension, hydrocarbon gas/liquid mixture flowing in a pipe with a diameter of order 1 m at elevated pressure, the equation of Azzopardi (1985) would give a Sauter mean diameter about 100 mm whilst that of Ambrosini *et al.* (1991) would yield a value of 1.5 mm. The Ambrosini result arrises from the effect of pipe diameter. Yet, the experimental data shows little effect of pipe diameter for diameters above 0.035 m. Obviously, more pertinent data is required to resolve this difference.

Ribeiro *et al.* (1995) found that their data for horizontal flows was best represented by the correlation of Azzopardi *et al.* (1980) for higher gas mass fluxes and by Ambrosini *et al.* (1991) at lower mass fluxes.

4.6. *Drop velocities*

The phase Doppler technique used by Azzopardi and Teixeira (1994) and the Ronchi grating technique employed by Fore and Dukler (1995a,b) provide simultaneous measurements of drop size and velocity. The results of both groups give similar trends. The effects of gas and liquid flow rates have been studied, at the centre line and at two intermediate radial positions. Figure 44 illustrates the mean drop velocities which show a similar radial distribution as the gas flow but their values are about 20% lower than those of the gas. The mean drop velocities on the centre line are approximately equal to the gas superficial velocity (figure 45). The distribution of velocities differs from a Gaussian as the peak is skewed towards the gas velocity. This follows from the fact that drops are created with very low velocities whilst there is an upper limit at the gas velocity.

There is a trend for smaller drops to be travelling at higher velocities† (figure 46). In addition, it can be seen that there is a wider range of velocities at smaller drop sizes. This can be explained by the fact that smaller drops will be most strongly affected by gas turbulence which can cause acceleration and deceleration in the lateral direction and so increase and decrease the time taken for drops to arrive at the probe volume and widen the range of axial velocities that they could achieve. Larger drops, being less susceptible to turbulence will show a narrower range of lifetimes and hence velocities.

The results of Azzopardi and Teixeira (1994) indicate that size and velocity are not strongly correlated. Their data show that the correlation coefficient, defined as

†Lopes and Dukler (1985) reported a contrary trend, larger drops having larger velocities.

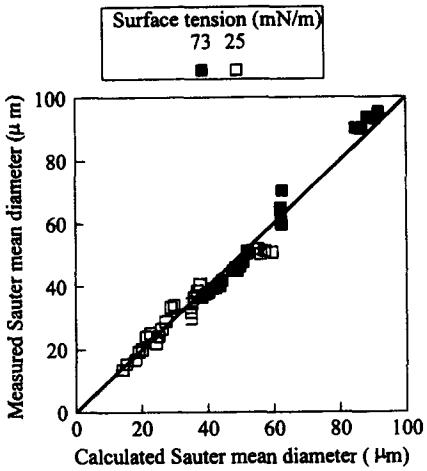

Figure 43. Test of equation of Ambrosini *et al.* (1991)—effect of surface tension.

$$r_c = \frac{\sum(u_{pi} - \bar{u}_p)\sum(D_i - D_{10})}{\left(\sum(u_{pi} - \bar{u}_p)^2 \sum(D_i - D_{10})\right)^{0.5}}, \qquad [22]$$

is small, negative and decreases in magnitude as the interface is approached. It also decreases with gas velocity and, in the centre of the channel, with liquid flow rate. These trends are in contrast to the results published by Lopes and Dukler (1985) who showed that drop velocity increased with size and had a positive correlation coefficient.

The spread in drop velocities, characterized by its normalized standard deviation, decreased with gas flow rate and distance from the wall (figure 47).

Lateral or transverse velocities have been reported by Andreussi and Azzopardi (1983), Wilkes *et al.* (1983b) and Lopes and Dukler (1985). The former two papers described results from the analysis of high speed cine film taken using the axial viewing technique developed by Hewitt and Whalley (1980). Because of the resolution of the system, measurements could only be made for drops of 250 μm and larger. Lopes and Dukler used a laser anemometry technique. The available measurements show that the lateral velocities of drops hardly change over their lifetime and show no dependence on drop size or direction of ejection from the liquid film. The experiments reported by Andreussi and Azzopardi and Wilkes *et al.* examined the effects of gas

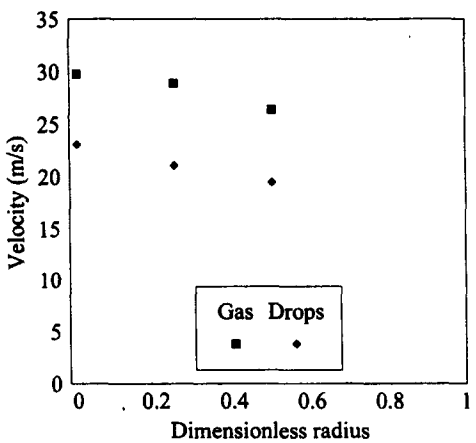

Figure 44. Radial variation of drop velocity: comparison with the local gas velocity (gas mass flux = 43.7 kg/m^{2}s; liquid mass flux = 15.9 kg/m^{2}s. (Based on figure from Two-phase Flow and Heat Transfer, HTD Vol. 197, Azzopardi and Teixeira, "Gas core turbulence and drop velocities in vertical annular two phase flow", pp. 37–46, Copyright (1994), with kind permission of ASME, New York, USA.)

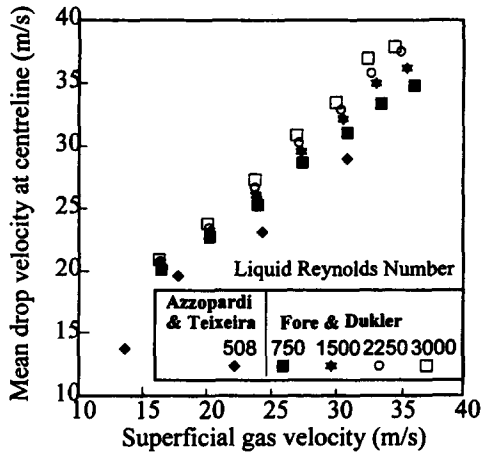

Figure 45. Mean centre line velocity for air/water. (Based on figure from Gas Liquid Flow in Fluid Mechanics and Heat Transfer, FED Vol. 244, Azzopardi *et al.*, "Entrained fraction in inclined annular gas/liquid flow", pp. 69–76, Copyright (1997), with kind permission of ASME, New York, USA.)

and liquid flow rates, gas density and tube diameter. Andreussi and Azzopardi argued that the transverse or ejection velocity was proportional to the friction velocity [$u^* = u_{gs}\sqrt{(f_i/2)}$] times the square root of the (gas to liquid) density ratio. Though this causes data from two gas densities to lie on the same line, Wilkes *et al.* showed that data from a smaller diameter tube lay on a different line. In an attempt to reconcile both sets of data, they have been plotted against a modified Weber number ($We^* = \rho_g u^{*2} D_t/\sigma$) (figure 48). Although this goes some way to drawing data together, it does not entirely describe the effect of tube diameter.

Transverse velocity data for horizontal annular flow has been reported by Azzopardi (1987). Values similar to those reported by Andreussi and Azzopardi (1983) were found though it is not so easy to reduce these data to the same basis as those for vertical flow.

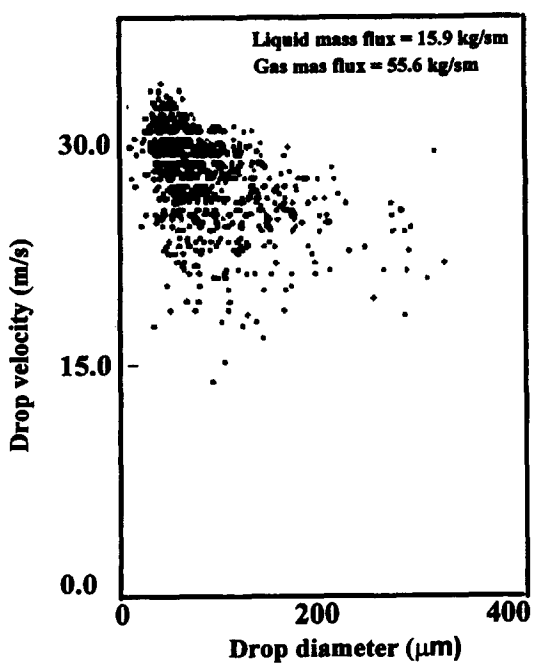

Figure 46. Effect of drop size on drop velocity—data from centre line. (Based on figure from Two-phase Flow and Heat Transfer, HTD Vol. 197, Azzopardi and Teixeira, "Gas core turbulence and drop velocities in vertical annular two phase flow", pp. 37–46, Copyright (1992), with kind permission of ASME, New York, USA.)

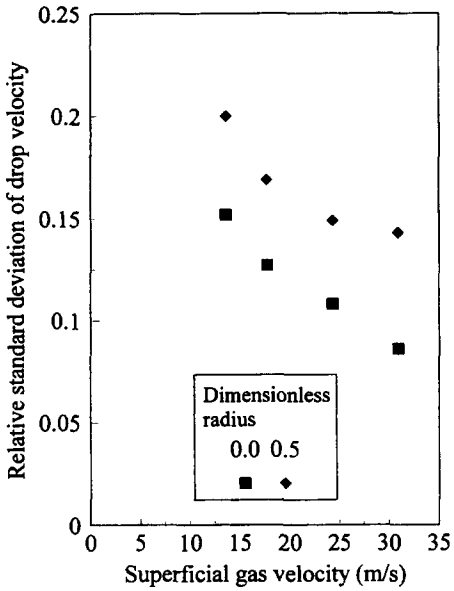

Figure 47. Effect of gas velocity on the relative standard deviation of drop velocity. (Based on figure from Two-phase Flow and Heat Transfer, HTD Vol. 197, Azzopardi and Teixeira, "Gas core turbulence and drop velocities in vertical annular two phase flow", pp. 37–46, Copyright (1992), with kind permission of ASME, New York, USA.)

4.7. *Turbulence*

In recent discussions of modelling of annular two-phase flow, Abolfadl and Wallis (1985) and Owen and Hewitt (1987) have suggested that knowledge of the turbulence within the drop-laden gas core might permit some of the empiricism to be removed. They propose that an effect of the presence of the drops is to suppress the level of turbulence in the gas core which would result in a modified log law for the velocity profile.

An examination of the published literature reveals that, apart from the data of Azzopardi and Teixeira (1994) discussed below, nothing has been published on turbulence in the gas core of annular flow. A small number of papers were found which report mean velocity profiles (Gill *et al.* 1964; Adorni *et al.* 1961; Subbotin *et al.* 1975; and Kirillov *et al.* 1978).

There is some information from other types of two-phase pipe flow. A recent review by Hetsroni (1989) reveals that measurements have been made of the continuous phase turbulence in both gas–solid and liquid–solid flows. Maeda *et al.* (1980), Lee and Durst (1982) and Tsuji and Morikawa (1982), Tsuji *et al.* (1984) have reported data for gas–solid flow whilst Zisselmar and Molerus (1979) investigated liquid–solid flows. From these it can be seen that turbulence

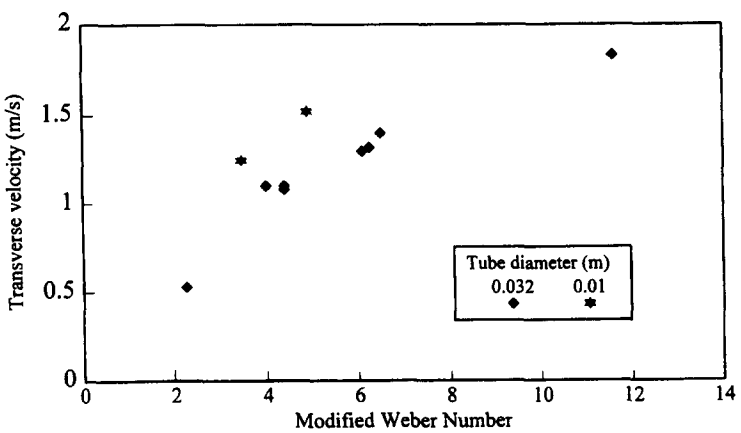

Figure 48. Dependence of transverse drop velocity on modified Weber number.

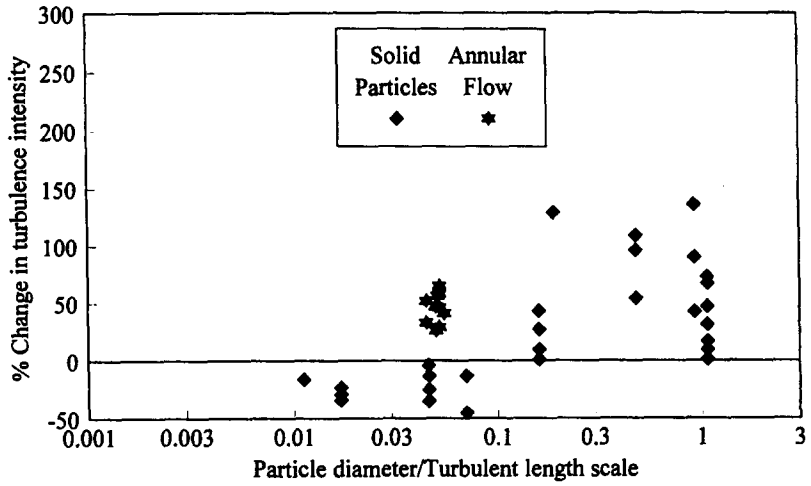

Figure 49. Change in turbulence intensity as a function of the length scale ratio. (Based on figure from Trans ASME, J. Fluids Engineering, Vol. 116, Azzopardi and Teixeira, "Detailed measurement of vertical annular flow—Part II: gas core turbulence", pp. 796–800, Copyright (1994), with kind permission of ASME, New York, USA.)

intensities can either increase or decrease from the single phase values. For smaller particles there is a suppression of turbulence, although the degree of suppression diminishes with particle concentration. For larger particles the turbulence intensity is enhanced the increase being directly dependent on concentration. Gore and Crowe (1989) show that these effects can be quantified by consideration of the ratio between particle size and a characteristic length scale of the turbulence. Ratios below 0.1 result in suppression; higher values correspond to an increase in turbulence. However, it must be remembered that these two-phase flows differ from annular flow in two fundamental aspects. Firstly, there is no liquid film present. In annular flow this can act as a rough wall. The second difference relates to steady state. Though this is achieved in the fluid–solid flows, in annular flow with its constant creation of drops from the film there can only be a dynamic steady state, i.e. there will always be freshly created drops present.

Measurements on gas phase turbulence in vertical annular flow have been made by Azzopardi and Teixeira (1994). They used a laser Doppler technique using light scattered from 1 μm polystyrene spheres inserted into the gas flow. This size had been chosen as calculations had shown that they would be good flow followers. Signals from these tracer particles were discriminated from those arising from drops by use of the amplitude as well as the visibility (ratio of AC to DC components—which is size dependent) of the Doppler bursts. Initially, measurements were made on single-phase gas flow to prove the technique.

The mean axial velocity profiles in both single and two-phase flow were found to fit an equation of the form:

$$\frac{u}{u_{MAX}} = \left(\frac{y}{R}\right)^{1/n}, \qquad [23]$$

where u_{MAX} is the maximum velocity in the channel, y is the distance from the wall and R is the tube radius. For annular flow, values of $1/n$ were larger than the equivalent single phase data values. However, when plotted against friction factor (determined from extrapolation of Reynolds stress data to provide wall shear stresses) the values of $1/n$ lie on the same line as data measured by Nikuradse (1932) and Nunner (1956) in rough walled pipes.

The relative change in the turbulence intensity of the gas ((value for two-phase flow minus the standard value)/standard value) is plotted against the ratio of drop size to characteristic turbulence length scale in figure 49 as suggested by Gore and Crowe (1989). The Sauter mean diameter was used as the characteristic drop size and the length scale was determined from the simple equation suggested by Hutchinson *et al.* (1971)—0.2 times the pipe radius. Length scales determined from the Reynolds stress and the gradient of the mean velocity profile gave similar

results. In contrast to those data from gas–solid and liquid–solid flows, the present data show that there was an increase in turbulence intensity above the standard value, even though the drop size–length scale ratio was below 0.1, probably for the reasons discussed above.

Further support for the idea that the increase in turbulence intensity is due to newly created drops is found if the increase in turbulence intensity plotted against the rate of entrainment. Increase in the amount of new drops increases the augmentation of turbulence.

Owen and Hewitt (1987) fitted published gas velocity profiles for annular flow using a universal-velocity-profile type logarithmic equation. They determined the friction velocity from pressure drop data. This resulted in unusual values for the von Karman constant. Owen and Hewitt found that the "two-phase" von Karman constant could be correlated by the ratio of the momentum of the gas to that of the gas core and attributed this to a suppression of turbulence. However, this is contrary to what has been measured. It could be argued that Owen and Hewitt analysed data from higher concentrations than those at which Azzopardi and Teixeira (1994) made measurements. Yet, if the increased turbulence is due to newly created drops, then the increase will be greater at higher concentration. This does not contradict Owen and Hewitt's finding, only their attributing the result to suppression of turbulence.

5. CONCLUSIONS ON DROP SIZES AND VELOCITIES

From the above it can be concluded that:

1. There is still a need to reconcile drop size data obtained by various groups. Though some suggestions have been put forward, there is still a need for a definitive study.
2. Drop size data have been gathered over reasonable ranges of parameters using the laser diffraction technique. It is supported by the results of other studies which used photography (Andreussi *et al.* 1978; Hay *et al.* 1996). This database permits trends to be determined. Although one or two equations give good predictive results, there are questions regarding their application to industrial cases.
3. In the mean, drops tend to have a velocity about 80% that of the gas. However, there is an upper limit—the maximum gas velocity. A lower limit is probably the velocity of waves. For lateral velocity there are data for large drops, more infromation is required for smaller ones.
4. Where it has been possible to measure them, turbulence intensities in annular flow show values higher than the equivalent single phase case. This increase is probably due to the high Reynolds numbers for newly created drops.

6. DEPLETION— DEPOSITION ONTO THE WALL FILM

6.1. *Methods of measurement*

There are two main techniques which have been used to measure the rate of deposition of drops onto the wall film. The first is that involving the measurement of the changes in concentration of a tracer injected into the film and described in the section on entrainment. Results using this technique have been reported by Jagota *et al.* (1973) and Schadel (1988) for upflow and by Leman *et al.* (1985) for downflow. In the second technique, the liquid film is extracted through a porous wall section and its flow rate measured. The liquid which deposits downstream of this point is determined by extracting the resulting film through a second porous wall section. Obviously, the technique is limited to cases where the liquid film flow rate formed by deposition remains below the critical value for the inception of entrainment. This technique was used by Cousins *et al.* (1965), Cousins and Hewitt (1968), Govan (1990) and Jepson (1992) for vertical upflow and Namie and Ueda (1972, 1973) for horizontal flow. It was also used by Ganic and Mastanaiah (1981) and El-Kassaby and Ganic (1986), although they did not create the drops by the shearing action of the gas on the film but by using a spray nozzle.

The simplest approach in the interpretation of deposition data considers it to be a mass transfer process, i.e. the rate of deposition is proportional to the difference in concentration between

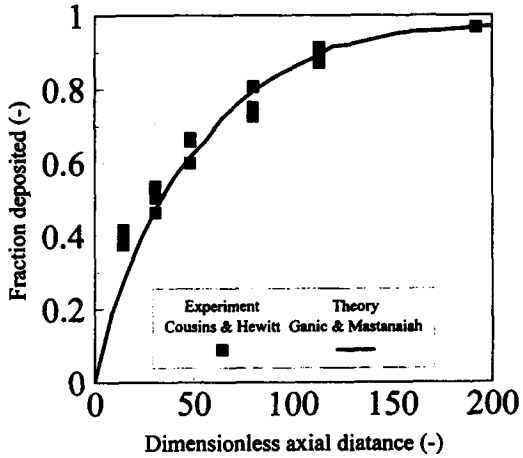

Figure 50. Comparison of the theory of Ganic and Mastanaiah (1981) with the data of Cousins and Hewitt (1968).

the concentration in the core, c, and that at the wall, c_o. If the interface can be assumed to be perfectly absorbing, i.e. $c_o = 0$, then

$$D = kc. \qquad [24]$$

The mass transfer coefficient, k, was originally taken as independent of the core drop concentration (Cousins and Hewitt 1968). Indications of the parametric dependence of k were given by McCoy and Hanratty (1977) and Papavergos and Hedley (1984). However, Namie and Ueda (1973), Andreussi and Zanelli (1976), Govan (1990), Schadel *et al.* (1990) and Jepson (1992) show that the mass transfer coefficient is dependent on the core concentration.

A number of models of the processes of deposition have been published. Many consider the process to be one of diffusive mass transport; the action of turbulence on drops is to make them move in a random manner. The simplest of these models (Hutchinson *et al.* 1971), considered uniform velocity and turbulence about the cross section. Ganic and Mastanaiah (1981) included the effect of gas velocity profile and Crane *et al.* (1983) allowed that there were radial profiles of gas mean velocity and turbulence. They also included the effects of collision and coalescence.

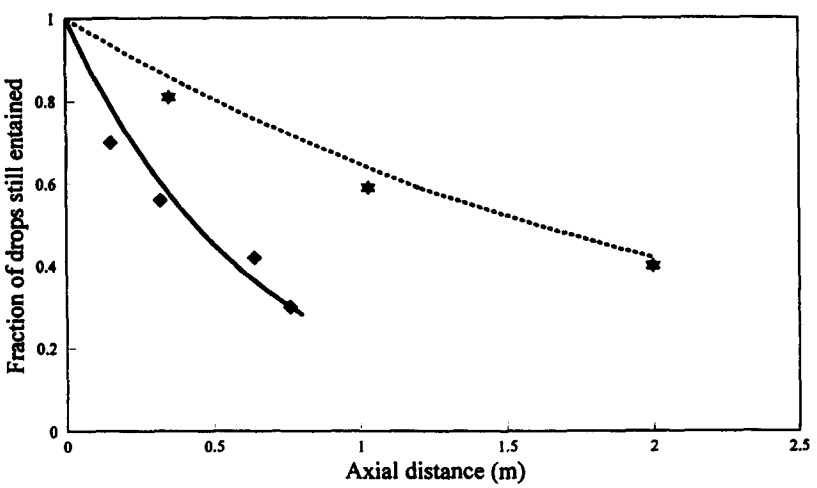

Figure 51. Comparison of the predictions of the numerical deposition model of Crane *et al.* (1983) with the data of Cousins and Hewitt (1968). (Based on figure from 1st Int. Conf. on Physical Modelling of Multiphase Flow, Crane *et al.*, "Numerical modelling of droplet deposition from vertical turbulent gas liquid flow", pp. 131–144, Copyright (1983), with kind permission of BHRA Fluid Engineering, Cranfield, UK.)

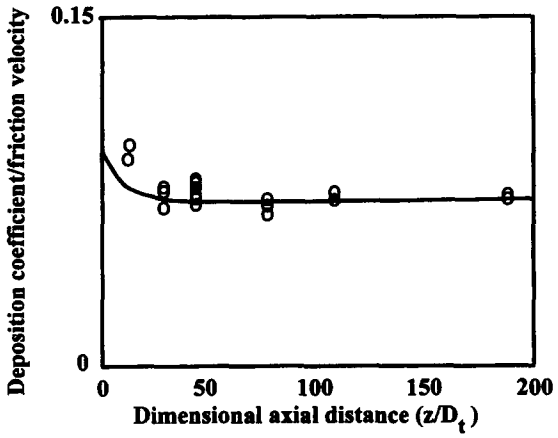

Figure 52. Comparison of the deposition constants measured by Cousins and Hewitt (1968) downstream of a film removal with the predictions of the model of Binder and Hanratty (1991).

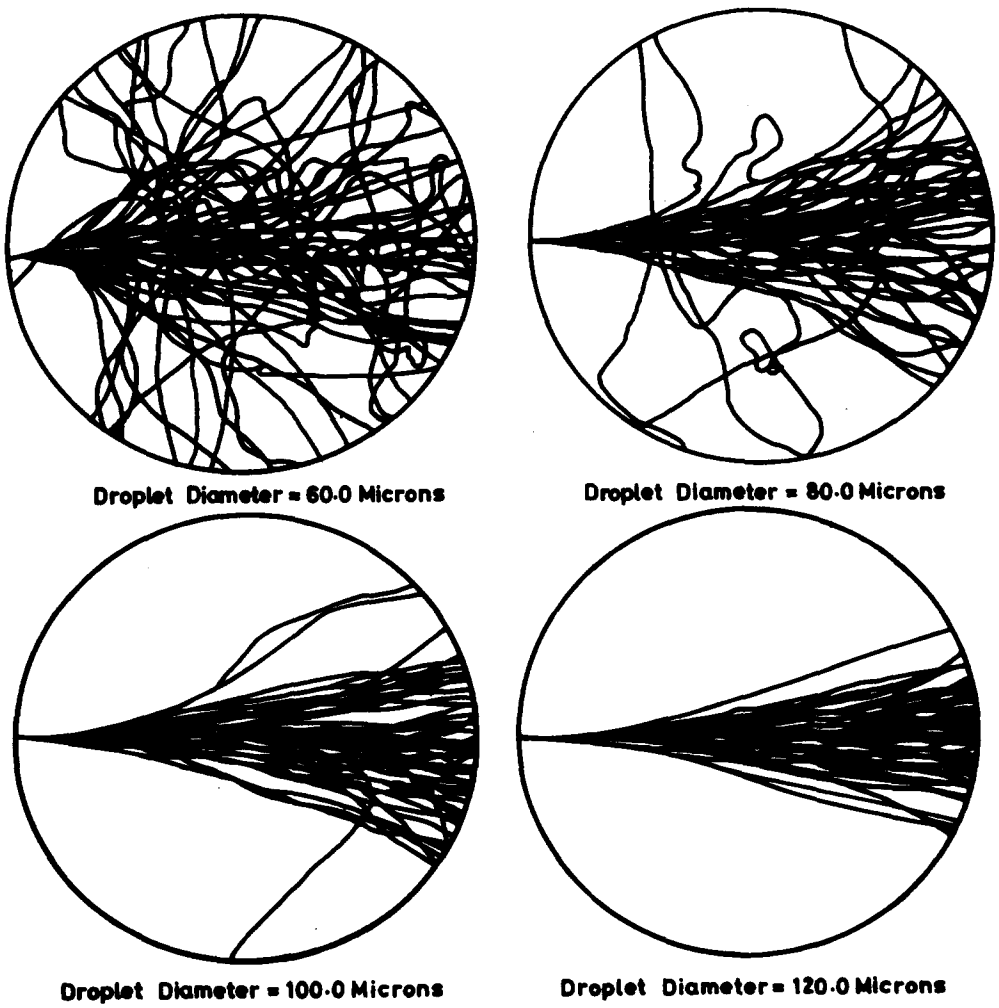

Figure 53. Simulation of drop motion (initial transverse velocity $v_i = 0.9$ m/s in all cases; Andreussi and Azzopardi, 1983).

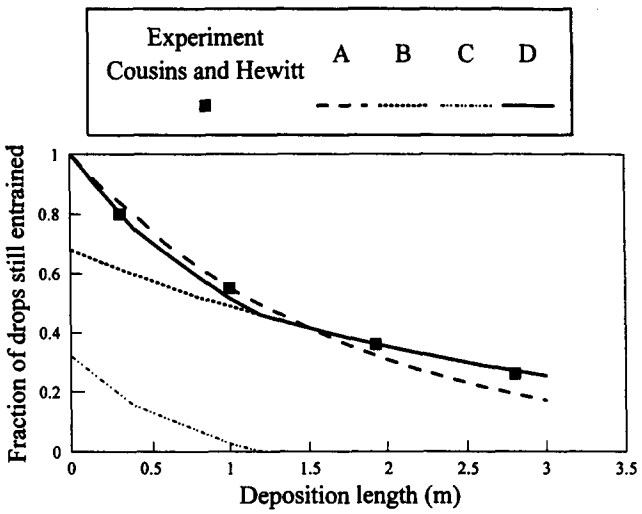

Figure 54. Prediction of the deposition data of Cousins and Hewitt (1968) by combined diffusion and direct impaction (James *et al.* 1980).

Further developments have been reported by Binder and Hanratty (1991), Hay *et al.* (1996) and Hanratty and Dykhno (1997). Hanratty and Dykhno (1997) give a review of latest ideas which consider that drops impact on surrounding surfaces by a free-flight mechanism. The depoosition rate is described by

$$R_d = Vc_W = \left(V\frac{c_W}{c_B}\right)c_B, \qquad [25]$$

where V is the average velocity of the drops, c_W is the mass concentration of drops at the wall and c_B is the bulk concentration. V can be related to the root mean square of the velocity fluctuations of the drops. As the drop concentration is radially uniform, $c_W/c_B = 1$, simplifying [25]. Hanratty and Dykhno (1997) discuss expressions for the root mean square of the velocity fluctuations of the drops.

Some of the models noted above have been compared with the data of Cousins and Hewitt (1968) (figures 50–52). Not surprisingly, they all show good agreement. Hewitt (1983), reviewing those models published by that date, noted that, faced with such a variety of accurate predictions, the question arises as to which is the correct one. He concludes that there are probably elements of truth in each one.

The interaction between drops and the gas (including turbulence) has been studied by a number of workers (e.g. James *et al.* 1980; Andreussi and Azzopardi 1983; Wilkes *et al.* 1983b; Reeks, 1977; and Uijttewaal and Oliemans, 1996). These use increasingly more complex models for the turbulence. The latest paper employs large eddy simulation (LES) and direct numerical simulation (DNS). There is are many publications about drop–gas interaction, although most are not specific to annular flow.

The concept that all drops are deposited by a diffusion-like mechanism was questioned by James *et al.* (1980), who employed the shadowgraphy technique of Hewitt and Whalley (1980) to observe drop behaviour. They reported that the (larger) drops that were visible did not move in a random manner but travelled across the cross section in straight lines. This was caused by the initial impetus given to the drop by the entrainment process. Calculations have been carried out which described the effect of turbulence by assuming that drops interact with a succession of eddies which move randomly about the cross section. The lateral motion of larger drops is unaffected whilst the motion of smaller ones appears more random (figure 53). James *et al.* the divided the depositing drops into two classes, those which landed by direct impaction and those which arrived by a diffusion-like process. Figure 54 shows that, while the fraction of drops remaining entrained after the film is removed (and entrainment ceases) could be fitted to the form of equation describing the diffusion process (A), the trend is not totally followed.

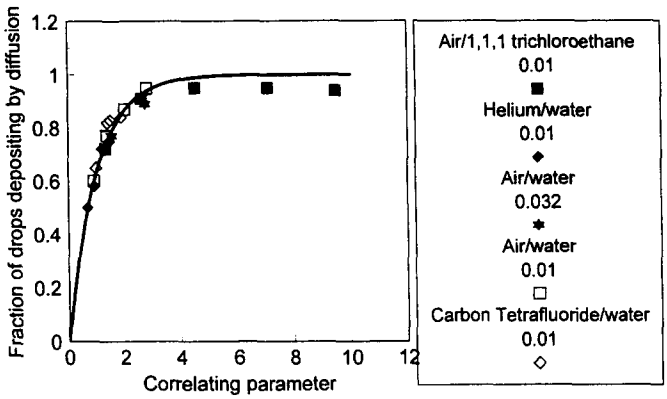

Figure 55. Correlation of fraction of drops depositing by diffusion. (Based on figure from Gas Liquid Flow in Fluid Mechanics and Heat Transfer, FED Vol. 244, Azzopardi *et al.*, "Entrained fraction in inclined annular gas/liquid flow", pp. 69–76, Copyright (1997), with kind permission of ASME, New York, USA.)

However, fitting a fraction of the drops by such an equation gives excellent agreement far from the film take-off point (B). Combining this with a simple trajectory model for the rest of the drops (C) gives the best overall agreement (D). Andreussi and Azzopardi (1983) developed this approach further and determined the fraction of drops depositing by diffusion for the then available data. Jepson (1992) extended this to a wider range of fluids from her own experiments. The results show that the direct impaction component is more important at low gas velocities, smaller tube diameters, lower densities and higher surface tension. Examination of the data and use of dimensional analysis results in a good correlation (figure 55), where the correlating curve is

$$F_D = 1 - e^{-\left[2.217 \frac{We^{1.42}}{Re_g^{0.89}} + 0.27\right]} \qquad [26]$$

where $We = (\rho_g u_{gs}^2 d_t)/\sigma$ and $Re_g = (\rho_g u_{gs} d_t)/\eta_g$.

Inspection of the equation indicates that the mechanism of direct impaction should be considered at conditions close to the transition to churn annular and for vacuum systems.

It is only possible to use this approach to analyse deposition data if there is reasonable certainty that there has been no re-entrainment from the film formed by deposition. This has precluded the use of data from higher liquid flow rates. However, Andreussi and Azzopardi (1983) have re-analysed measurements from tracer studies using this concept and found that there is a change in the slope of the concentration/axial position plot. This they attribute to the existence of two deposition mechanisms, an effect which disappeared at high gas velocities (where [26] would suggest that all drops deposit by a diffusion-like mechanism) and liquid flow rates.

The effect of liquid flow rate has been examined by Hay *et al.* (1996). They determined that for the theoretical approach of Binder and Hanratty (1991) to give accurate predictions required the root mean square lateral drop velocity to decrease significantly with drop concentration. They postulate that this might occur with the decrease in velocity being an effect of drop coalescence, a processes for whose occurrence there is strong evidence. This last point has been studied theoretically by Soldati and Andreussi (1996). Their predictions correctly follow the trends in deposition mass transfer coefficient with liquid flow rate.

7. CONCLUSIONS ON DEPOSITION

From the above it can be concluded that:

1. Deposition is best measured by a tracer interchange technique.
2. There are very encouraging developments in the modelling of deposition.
3. For certain conditions, the initial velocity of the drops is important and predominates throughout its entire flight.

REFERENCES

Abolfadl, M. A. (1984) Analysis of annular two-phase flow with liquid entrainment. Ph.D. Thesis, Thayer School of Engineering, Dartmouth College, U.S.A.

Abolfadl, M. and Wallis, G. B. (1985) A mixing length model for annular two phase flow.. *Phys.-Chem. Hydrodyn.* **6,** 49–68.

Addison, C. C. (1945) The properties of freshly formed surfaces: Part IV—the influence of chain length and structure on the static and dynamic surface tensions of aqueous alcoholic solutions. *J. Chem. Soc.*, 98–106.

Adorni, N., Casagrande, I., Cravarolo, L., Hassid, A. and Silvestri, M. (1961) Experimental data on two-phase flow: liquid film thickness, phase and velocity distribution, pressure drops in vertical gas–liquid flow. C.I.S.E. report no. R35.

Ambrosini, W., Andreussi, P. and Azzopardi, B. J. (1991) A physically based correlation for drop size in annular flow. *Int. J. Multiphase Flow* **17,** 497–507.

Andreussi, P. (1983) Droplet transfer in two-phase annular flow. *Int. J. Multiphase Flow* **9,** 697–713.

Andreussi, P. and Azzopardi, B. J. (1983) Droplet deposition and interchange in annular gas–liquid flow. *Int. J. Multiphase Flow* **9,** 681–695.

Andreussi, P. and Zanelli, S. (1976) Liquid phase mass transfer in annular gas–liquid flow. *Ing. Chim. Ital.* **12,** 132–136.

Andreussi, P. and Zanelli, S. (1978) Downwards annular-mist flows of air–water mixtures. *Int. Seminar*, Dubrovnik, September 4–9. Sponsored by ICHMT.

Andreussi, P., Romano, G. and Zanelli, S. (1978) Drop size distribution in annular mist flow. *First Conf. on Liquid Atomisation in Spray Systems*, Tokyo, August 27–31.

Andreussi, P., Asali, J. C. and Hanratty, T. J. (1985) Initiation of roll waves in gas–liquid flows. *A.I.Ch.E.J.* **31,** 119–126.

Andritsos, N. (1992) Statistical analysis of waves in horizontal stratified gas–liquid flow. *Int. J. Multiphase Flow* **18,** 465–473.

Arnold, C. R. and Hewitt, G. F. (1967) Further developments in the photography of two-phase gas– liquid flow. *J. Phot. Sci.* **15,** 97–114.

Asali, J. C. (1984) Entrainment in vertical gas–liquid annular flows. Ph.D. Thesis, University of Illinois, Urbana, IL.

Asali, J. C., Hanratty, T. J. and Andreussi, P. (1985) Interfacial drag and film height for vertical annular flow. *AIChE J.* **31,** 895–902.

Azzopardi, B. J. (1979) Measurements of drop sizes. *Int. J Heat Mass Transfer* **22,** 1245–1279.

Azzopardi, B. J. (1983) Mechanisms of entrainment in annular two-phase flow. UKAEA Report AERE-R 11068.

Azzopardi, B. J. (1984) A diffraction drop sizing technique: its testing and application to confined sprays. *Filtrat. Separat.* **21,** 415–419.

Azzopardi, B. J. (1985) Drop-sizes in annular two-phase flow. *Exp. Fluids* **3,** 53–59.

Azzopardi, B. J. (1986) Disturbance wave frequencies, velocities and spacing in vertical annular two-phase flow. *Nucl. Engng Des.* **92,** 121–133.

Azzopardi, B. J. (1987) Observations of drop motion in horizontal annular flow. *Chem. Engng Sci.* **42,** 2059–2062.

Azzopardi, B. J. (1992) Instrumentation for particle size analysis by far field diffraction: accuracy, limitations and future. In Particle Size Analysis, ed. N. G. Stanley-Wood and R. W. Lines. Royal Society of Chemistry, Cambridge.

Azzopardi, B. J. (1994) The split of vertical annular flow at a large diameter T junction. *Int. J. Multiphase Flow* **20,** 1071–1083.

Azzopardi, B. J. and Gibbons, D. B. (1983) Annular two-phase flow in a large diameter tube. *Chem. Eng.* **398,** 19–31.

Azzopardi, B. J. and Hewitt, G. F. (1998) Maximum drop sizes in gas–liquid flows. *Multiphase Sci. Tech.*, accepted.

Azzopardi, B. J. and Hibberd, S. (1994) Determination of maximum drop sizes in annular gas/liquid flow. *Proc. 6th Int. Conf. on Liquid Atomization and Spray Systems*, pp. 962–969.

Azzopardi, B. J. and Whalley, P. B. (1980) Artificial waves in annular two-phase flow. *ASME Winter Annual Meeting*, Chicago, Published in *Basic Mechanisms in Two-Phase Flow and Heat-Transfer*, pp. 1–8.

Azzopardi, B. J. and Zaidi, S. H. (1997) The effect of inclination on drop sizes in annular gas–liquid flow. *Exp. Heat Transfer Fluid Mech. Thermodyn., Ed. ETS* **2,** 1167–1174.

Azzopardi, B. J., Freeman, G. and Whalley, P.B. (1978) Drop sizes in annular two-phase flow. *ASME Winter Annual Meeting*, Published in *Topics in Two-phase Flow and Heat Transfer*, pp. 165–173.

Azzopardi, B. J., Fryer, P. J. and Freeman, G. (1979) The frequency of disturbance waves in annular two-phase flow. UKAEA Report AERE R9347.

Azzopardi, B. J., Freeman, G. and King, D. J. (1980) Drop sizes and deposition in annular two-phase flow. UKAEA Report AERE R9634.

Azzopardi, B. J., Taylor, S. and Gibbons, D. B. (1983) Annular two-phase flow in large diameter pipes. *Int. Conf. on Physical Modelling of Multi-Phase Flow*, April 19–21, Coventry, pp. 267–282.

Azzopardi, B. J., Teixeira, J. C. F. and Jepson, D. M. (1989) Drop sizes and velocities in vertical annular two-phase flow. *Proc. Int. Conf. on Mechanics of Two-phase Flows*, Taipei, Taiwan, pp. 261–266.

Azzopardi, B. J., Piearcey, A. and Jepson, D. M. (1991) Drop size measurements for annular two-phase flow in a 20 mm diameter vertical tube. *Exp. Fluids* **11,** 191–197.

Azzopardi, B. J., Zaidi, S. H. and Sudlow, C. (1996) The effect of inclination on drop sizes in annular gas–liquid flow. *Eur. Two-phase Flow Group Meeting*, Grenoble, June 3–5, Paper E1.

Azzopardi, B. J., Zaidi, S. H. and Jepson, D. M. (1997) Entrained fraction in inclined annular gas/liquid flow. *Gas Liquid Flow in Fluid Mechanics and Heat Transfer*, ASME FED **244,** 69–76.

Bennett, A. W., Hewitt, G.F., Kearsey, H.A., Keeys, R.K.F. and Stinchcombe, R.A. (1969) Measurement of liquid film flow rates at 1000 psi in upward steam water flow in a vertically heated tube. UKAEA Report AERE R5809.

Binder, J. L. and Hanratty, T. J. (1991) A diffusion model for droplet dispersion in gas/liquid annular flow. *Int. J. Multiphase Flow* **17,** 1–11.

Bowen, I. G. and Davies, G. P. (1951) Particle size distribution and the estimation of Sauter mean diameter. Shell Technical Report No. ICT/28.

Brazier, K., Gillespie, R. F., Dalzell, W. and Livesley, D. M. (1988) Bias corrections to size distribution and concentrations in phase-Doppler particle measurement. UKAEA Report AERE R13270.

Brown, D. J. (1978) Disequilibrium annular flow. D.Phil. Thesis, University of Oxford.

Brown, D. J., Jensen, A. and Whalley, P.B. (1975) Non-equilibrium effects in heated and unheated annular two-phase flow. ASME Paper 75-WA/HT/7.

Cao, J., Brown, D. J. and Rennie, A. G. (1991) Laser diffraction particle sizing in dense suspensions and sprays with correction for multiple scattering. *J. Inst. Energy* **64,** 26–30.

Crane, R. I., Farwagi, S. and Williams, A. J. E. (1983) Numerical modelling of droplet deposition from vertical turbulent gas flow. *Proc. Int. Conf. on Physical Modelling of Multi-phase Flow*, Coventry.

Cousins, L. B. and Hewitt, G.F. (1968) Liquid phase mass transfer in annular two-phase flow: droplet deposition and liquid entrainment. UKAEA Report AERE-R5657.

Cousins, L.B., Denton, W. H. and Hewitt, G. F. (1965) Liquid mass transfer in annular two-phase flow. *Proc. Symp. Two-phase Flow*, Vol. 2, paper C4, Exeter.

Dodge, L. G. (1984) Calibration of the Malvern particle sizer. *Appl. Opt.* **23,** 2415; Change of calibration of diffraction-based particle sizes in dense sprays. *Opt. Engng* **23,** 626–630.

Dressler, R. F. (1949) Mathematical solution of the problem of roll-waves in inclined open channels. *Commun. Pure Appl. Math.* **2,** 149–194.

El-Kassaby, M. M. and Ganic, E. N. (1986) Droplet deposition in two-phase turbulent flow. *Int. J. Heat Mass Transfer* **29,** 1149–1158.

Felton, P. G., Hamidi, A. A. and Aigai, A. K. (1985) Measurement of drop size distribution in dense sprays by laser diffraction. *3rd Int. Conf. on Liquid Atomization and Spray Systems*, London. Institute of Energy, London.

Fore, L. B. and Dukler, A. E. (1995a) The distribution of drop size and velocity in gas–liquid annular flow. *Int. J. Multiphase Flow* **21,** 137–149.

Fore, L. B. and Dukler, A. E. (1995b) Droplet deposition and momentum transfer in annular flow. *AIChE J.* **41,** 2040–2046.

Fukano, T., Ousaka, A., Morimoto, T. and Sekoguchi, K. (1983) Air–water annular two-phase flow in a horizontal tube (Part II: circumferential variation of film thickness parameters). *Bull. JSME* **26,** 1387–1395.

Ganic, E. N. and Mastanaiah, K. (1981) Investigation of droplet deposition from turbulent gas streams. *Int. J. Multiphase Flow* **7,** 401–422.

Gibbons, D. B. (1985) Drop formation in annular two-phase flow. Ph.D. Thesis, University of Birmingham.

Gibbons, D. B., Azzopardi, B. J. and Bott, T. R. (1983) Laser tomographic investigation of the entrained liquid in annular two-phase flow. *Int. Conf. Physical Modelling of Multiphase Flow*, pp. 327–336.

Gibbons, D. B., Azzopardi, B. J. and Bott, T. R. (1985) Determination of the rate of entrainment in annular two-phase flow. *2nd Int. Conf. on Multiphase Flow*, London, June 19–21.

Gill, L. E., Hewitt, G. F. and Lacey, P. M. C. (1964) Sampling probe studies of the gas core in annular two-phase flow: II, studies of the effect of phase flowrates on phase and velocity distributions. *Chem Engng Sci.* **19,** 665–682.

Gill, L. E., Hewitt, G. F. and Lacey, P. M. C. (1968) Sampling probe studies of the gas core in annular two-phase flow: III, distribution of velocity and droplet flowrate after injection through a centre jet. *Chem Engng Sci.* **23,** 677–686.

Gill, L. E., Hewitt, G. F. and Roberts, D. N. (1969) Studies of the behaviour of disturbance waves in a long vertical tube. UKAEA Report AERE R6012.

Gore, R. and Crowe, C. T. (1989) Effects of particle size on modulating turbulence intensity. *Int. J. Multiphase Flow* **15,** 279–285.

Govan, A. H. (1990) Modelling of vertical annular and dispersed two-phase flows. Ph.D. Thesis, Imperial College, London.

Govan, A. H., Hewitt, G. F., Owen, D. G. and Bott, T. R. (1988) An improved CHF modelling code. *2nd UK National Heat Transfer Conf.*, Strathclyde.

Hall Taylor, N. S. (1966) Interfacial wave phenomena in vertical annular two-phase flow. Ph.D. Thesis, University of Cambridge.

Hall Taylor, N. S. and Nedderman, R. M. (1968) The coalescence of disturbance waves in annular two-phase flow. *Chem. Engng Sci.* **23,** 551–564.

Hall Taylor, N. S., Hewitt, G. F. and Lacey, P. M. C. (1963) The motion and frequency of large disturbance waves in annular two-phase flow of air–water mixtures. *Chem Engng Sci.* **18,** 537–552.

Hamidi, A. A. and Swithenbank, J. (1986) Treatment of multiple scattering of light in laser diffraction measurement technique in dense sprays and particle fields. *J. Inst. Energy* **59,** 101–105.

Hammond, D.C. (1980) Accuracy verification of a Malvern ST 1800 Analyser. General Motors Report GMR 3195.

Hanratty, T. J. and Dykhno, L. A. (1997) Physical issues in analyzing gas–liquid annular flows. *Exp. Heat Transfer Fluid Mech. Thermodyn. Ed. ETS* **2,** 1127–1136.

Hawkes, N. J. and Hewitt, G. F. (1995) Experimental studies of wispy-annular flow. *Int. Conf. on Two-phase Flow Modelling and Experimentation*, Rome, 9–11 October.

Hay, K. J., Liu, Z. C. and Hanratty, T. J. (1996) Relation of deposition rates to drop size at large concentrations. *Int. J. Multiphase Flow* **22,** 829–848.

Henstock, W. H. and Hanratty, T. J. (1976) The interfacial drag and height of the wall layer in annular flow. *AIChE J.* **22,** 990–1000.

Hetsroni, G. (1989) Particles–turbulence interaction. *Int. J. Multiphase Flow* **15,** 735–746.

Hewitt, G. F. (1962) Unpublished information.

Hewitt, G. F. (1983) Detailed modelling of two phase flow and its application to system prediction. *Proc. 2nd Int Topical Meeting on Nuclear Reactor Thermal-Hydraulics (ANS/ASME/AIChE)*, Vol. 1, pp. 38–48.

Hewitt, G. F. and Lovegrove, P. C. (1969) Frequency and velocity measurements of disturbance waves in annular two-phase flow. UKAEA Report AERE R4304.

Hewitt, G. F. and Nicholls, B. (1969) Film thickness measurements in annular two-phase flow using a fluorescence spectrometer technique UKAEA Report, AERE-R4506.

Hewitt, G. F. and Whalley, P. B. (1980) Advanced optical instrumentation methods. *Int. J. Multiphase Flow* **6,** 139–156.

Hills, J. H. (1997) The critical liquid flow rates for wave and droplet formation in annular gas–liquid flow. *Exp. Heat Transfer Fluid Mech. Thermodyn., Ed. ETS* **2,** 1241–1247.

Hirleman, E. D. (1989) A general solution to the inverse near-forward scattering particle sizing problem in multiple scattering environments: theory. *Proc. 2nd Int. Congress on Optical Particle Sizing*, Tempe, AZ, pp. 159–168.

Hirleman, E. D. and Dodge, L. G. (1985) Performance comparison of Malvern instruments laser diffraction drop size analyser. *3rd Int. Conf. on Liquid Atomization and Spray Systems*, London. Institute of Energy, London.

Hirleman, E. D., Oechsle, V. and Chigier, N. A. (1984) Response characteristics of laser diffraction particle size analyzers: optical sample volume extent and lens effects. *Opt. Engng* **23,** 610–619.

Holt, A. J. and Azzopardi, B. J. (1995) Two-phase pressure drop and void fraction relevant to compact two-phase heat exchangers. *Proc. 4th U.K. National Heat Transfer Conf.*, Manchester, September 26–27, pp. 437–441. I.Mech.E., London.

Hutchinson, P. and Whalley, P. B. (1973) A possible characterisation of entrainment in annular flow. *Chem. Engng Sci.* **28,** 974–975.

Hutchinson, P., Hewitt, G. F. and Dukler, A. E. (1971) Deposition of liquid or solid dispersion from turbulent gas streams: a stochastic model. *Chem. Engng Sci.* **26,** 419–439.

Ishii, M. and Grolmes, M. A. (1975) Inception criteria for droplet entrainment in two-phase concurrent flow. *AIChE J.* **21,** 308–318.

Jagota, A. K., Rhodes, E. and Scott, D. S. (1973) Tracer measurements in two-phase annular flow to obtain interchange and entrainment. *Can. J. Chem. Engng* **51,** 139–148.

James, P. W., Hewitt, G. F. and Whalley, P. B. (1980) Droplet motion in two phase flow. *Proc. ANS/ASME/NRC IntTopical Meeting on Nuclear Reactor Thermal-Hydraulics*, Vol. 2, pp. 1484–1503.

Jayanti, S., Hewitt, G. F. and White, S. P. (1990) Time-dependent behaviour of the liquid film in horizontal annular flow. *Int. J. Multiphase Flow* **16,** 1097–1116.

Jepson, D. M. (1992) Vertical annular flow: the effect of physical properties. D.Phil. Thesis, University of Oxford.

Jepson, D. M., Azzopardi, B. J. and Whalley, P. B. (1989) The effect of gas properties on drops in annular flow. *Int. J. Multiphase Flow* **15,** 327–339.

Jepson, D. M., Azzopardi, B. J. and Whalley, P. B. (1990) The effect of physical properties on drop size in annular flow. In *9th Intl Heat Transfer Conf.*, Jerusalem, Vol. 6, pp. 95–100.

Jurman, L. A., Bruno, K. and McCready, M. J. (1989) Periodic and solitary waves on thin, horizontal, gas-sheared liquid films. *Int. J. Multiphase Flow* **15,** 371–384.

Kataoka, I., Ishii, M. and Mishima, K. (1983) Generation and size distribution of droplet in annular two-phase flow. *Trans ASME J. Fluids Engng* **105,** 230–238.

Kirillov, P. L., Smogalev, I. P., Suvurov, M. Y., Shumsky, R. V. and Stein, Y. Y. (1978) Investigation of steam–water flow characteristics at high pressures. *Proc. 6th IntHeat Transfer Conf.*, Toronto, Canada, Vol. 1, pp. 315–320.

Kocamustafaogullari, G., Smits, S. R., Razi, J. and Huang, W. D. (1993) Droplet size modelling in annular flow. *Proc. 6th Int. Topical Meeting on Nuclear Reactor Thermal Hydraulics*, Grenoble, October 5–8, Vol. 2, pp. 1021–1030.

Lee, S. L. and Durst, F. (1982) On the motion of particles in turbulent duct flows. *Int. J. Multiphase Flow* **8,** 125–146.

Leman, G. W., Agostini, M. and Andreussi, P. (1985) Tracer analysis of developing two-phase annular flow. *Physiochem. Hydrodyn.* **6,** 223–237.

Linstead, R. D., Evans, D. L., Cass, J. and Smith, R. V. (1978) Private communication.

Lopes, J. C. B. and Dukler, A. E. (1985) Droplet sizes, dynamics and deposition in vertical annular flow. US Nucl. Regulatory Commission, Washington DC, USA, Report NUREG/CR-4424.

Maeda, M., Hishida, K. and Furutani, T. (1980) Optical measurements of local gas and particle velocity in an upward flowing gas–solid suspension. In *Polyphase Flow and Transport Technology*, Century 2_ETC, San Franciso, CA, p. 211.

Martin, C. J. (1983) Annular two-phase flow. D.Phil. Thesis, University of Oxford.

Martin, C. J. and Azzopardi, B. J. (1985) Waves in vertical annular flow. *Physiochem. Hydrodyn.* **6,** 257–265.

Mayinger, F. and Zetzmann, K. (1976) Flow patterns of two-phase flow in inside-cooled tubes; a generalised flow pattern map based on investigation in water and freon. Advanced Study Institute in Two-phase Flow and Heat Transfer, Istanbul.

McCoy, D. D. and Hanratty, T. J. (1977) Rate of deposition of droplets in annular two-phase flow. *Int. J. Multiphase Flow* **3,** 319–331.

McVean, S. S. and Wallis, G. B. (1969) Experience with the Wicks–Dukler probe for measuring drop size distributions in sprays. Report, Dartmouth College, Hanover, NH.

Miloshenko, V. I., Nigmatulin, B. I., Petukhov, V. V. and Trubkin, N. I. (1989) Burnout and distribution of liquid in evaporative channels of various lengths. *Int. J. Multiphase Flow* **15,** 393–401.

Miya, M., Woodmansee, D. E. and Hanratty, T. J. (1971) A model for roll waves in gas–liquid flow. *AIChE J.* **26,** 1915–1931.

Mugele, R. A. and Evans, H. D. (1951) Droplet size distribution in sprays. *Ind. Engng Chem.* **43,** 1317–1324.

Namie, S. and Ueda, T. (1972) Droplet transfer in two-phase annular mist flow: Part 1, Experiment of droplet transfer rate and distribution. *Bull. JSME* **15,** 1568–1580.

Namie, S. and Ueda, T. (1973) Droplet transfer in two-phase annular mist flow: Part 2, Predictions of droplet transfer rate. *Bull. JSME* **16,** 752–764.

Nedderman, R. M. and Shearer, C. J. (1963) The motion and frequency of large disturbance waves in annular two-phase flow of air–water mixtures. *Chem. Engng Sci.* **18,** 661–670.

Nigmatulin, R. I. (1991) *Dynamics of Multiphase Media*, Vol. 2, Sect. 7. Hemisphere, Washington, DC.

Nigmatulin, R. I., Nigmatulin, B. I., Khodzaev, Y. A. and Kroshilin, V. E. (1996) Entrainment and deposition rates in a dispersed-film flow. *Int. J. Multiphase Flow* **22,** 19–30.

Nikuradse, J. (1932) Gesetzmassigkeiten der turbulenten Stromung in glatten Rohren. VDI-Forschungsheft 356.

Nunner, W. (1956) Waermeubergang und Druckfall in rauhen Rohren. VDI-Forschungsheft 455.

Ohba, K. and Nagae, K. (1993) Characteristics and behaviour of the interfacial wave on the liquid film in a vertically upward air–water two-phase annular flow. *Nucl. Engng Des.* **141,** 17–25.

Okada, O., Fujimatsu, T., Fujita, H. and Homma, K. (1994) Some problems on droplet size measurement by immersion liquid method. *Proc. 6th Int. Conf. on Liquid Atomization and Spray Systems*, pp. 406–413.

Okada, O., Fujimatsu, T., Fujita, H. and Nakajima, Y. (1995) Measurement of droplet size distribution in an annular mist flow in a vertical pipe by immersion liquid method. *Proc. 2nd., Int. Conf on Multiphase Flow*, Kyoto, Vol. 1, pp. IP2/11–IP2/18.

Owen, D. G. and Hewitt, G. F. (1984) A proposed entrainment correlation. UKAEA Report AERE R12279.

Owen, D. G. and Hewitt, G. F. (1987) An improved annular two-phase flow model. *Proc. 3rd Int. Conf. on Multiphase Flow*, The Hague, Paper C1.

Papavergos, P. G. and Hedley, A. B. (1984) Particle deposition behaviour from turbulent flows. *Trans Inst. Chem. Engng* **62A,** 275–295.

Paras, S. V. and Karabelas, A. J. (1991) Properties of the liquid layer in horizontal annular flow. *Int. J. Multiphase Flow* **17,** 439–454.

Paras, S. V., Vlachos, N. A. and Karabelas, A. J. (1994) Liquid layer characteristics in stratified-atomization flow. *Int. J. Multiphase Flow* **20,** 939–956.

Pashniak, D. W. (1969) An investigation of the interfacial disturbances in vertical two phase flow. Ph.D. Thesis, University of Washington.

Pearce, D. L. (1979) Film waves in horizontal annular flow: space–time correlator experiments. CEGB Report No. CERL/RD/L/N 193/75.

Pogson, J. T., Roberts, J. H. and Waibler, P. J. (1970) An investigation of the liquid disintegration in annular mist flow. *Trans. ASME, J. Heat Transfer* **92,** 651–658.

Pols, R. M., Azzopardi, B. J. and Hibberd, S. (1996) Roll waves in inclined co-current separated gas–liquid flow. *Eur. Two-phase Flow Group Meeting*, Grenoble, June 3–5, Paper F3.

Quandt, E. R. (1965) Measurements of some basic parameters in two-phase annular flow. *AIChE J.* **11,** 311–318.

Rea, S. and Azzopardi, B. J. (1996) Two phase flow at T-junctions. *Eur. Two-phase Flow Group Meeting*, Grenoble, June 3–5, Paper G2.

Reeks, M. W. (1977) On the dispersion of small particles suspended in an isentropic turbulence. *J. Fluid Mech.* **83,** 529–546.

Ribeiro, A. M., Bott, T. R. and Jepson, D.M. (1995) Drop size and entrainment measurements in horizontal flow. *Int. Conf. on Two-phase Flow Modelling and Experimentation*, Rome, October 9–11.

Rosin, P. and Rammler, E. (1933) Laws governing the fineness of powdered coal. *J. Inst. Fuel* **7,** 29–36.

Sawai, T., Yamauchi, S. and Nakanishi, S. (1989) Behaviour of disturbance waves under hydrodynamic non-equilibrium conditions. *Int. J. Multiphase Flow* **15,** 341–356.

Schadel, S. A. (1988) Atomisation and deposition rates in vertical annular two-phase flow. Ph.D. Thesis, University of Illinois, Urbana-Champaign, IL.

Schadel, S. A. and Hanratty, T. J. (1989) Interpretation of atomisation rates of the liquid film in gas– liquid annular flow. *Int. J. Multiphase Flow* **15,** 893–900.

Schadel, S. A., Leman, G. W., Binder, J. L. and Hanratty, T. J. (1990) Rates of atomisation and deposition in vertical annular flow. *Int. J. Multiphase Flow* **16,** 363–374.

Sekoguchi, K. and Takeishi, M. (1989) Interfacial structures in upward huge wave flow and annular flow regimes. *Int. J. Multiphase Flow* **15,** 295–305.

Sekoguchi, K. and Mori, K. (1997) New development of experimental study on interfacial structure in gas–liquid two-phase flow. *Exp. Heat Transfer Fluid Mech. Thermodyn., Ed. ETS* **2,** 1177–1188.

Sekoguchi, K., Nishikawa, K., Nakasatomi, M., Nishi, H. and Kaneugi, A. (1973) Trans. JSME **39,** 313.

Semiat, R. and Dukler, A. E. (1981) Simultaneous measurement of size and velocity of bubbles and drops: a new optical technique. *AIChE J.* **27,** 148–159.

Sevik, M. and Park, S. H. (1973) The splitting of drops and bubbles by turbulent fluid flow. *Trans. ASME J. Fluids Engng* **95,** 53–60.

Shearer, C. J. (1964) Interfacial wave phenomena in two-phase flow. Ph.D. Thesis, University of Cambridge.

Soldati, A. and Andreussi, P. (1996) The influence of coalescence on droplet transfer in vertical annular flow. *Chem. Engng Sci.* **51,** 353–363.

Subbotin, V. I., Kirillov, P. L., Smogalev, I. P., Suvorov, M. Y., Stein, Y. Y. and Shumsky, R. V. (1975) Measurement of some characteristics of a steam–water flow in a round tube at pressures of 70 and 100 atm. A.S.M.E. paper No. 75-WA/HT-21.

Swithenbank, J., Beer, J. M., Taylor, D. S., Abbot, D. and McCreath, G. C. (1976) A laser diagnostic for the measurement of droplet and particle size distributions. *Prog. Astronaut. Aeronaut.* **1,** 421–447.

Tatterson, D. F. (1975) Rates of atomization and drop size in annular two-phase flow. Ph.D. Thesis, University of Illinois, Urbana, IL.

Tatterson, D. F., Dallman, J. C. and Hanratty, T. J. (1977) Drop sizes in annular gas–liquid flows. *AIChE J.* **23,** 68–76.

Tayali, N. E. and Bates, C. J. (1990) Particle sizing techniques in multiphase flow: a review. *Flow Meas. Instrum.* **1,** 77–105.

Tayali, N. E., Bates, C. J. and Yeoman, M. L. (1990) Drop size and velocity measurements in vertical developing annular two-phase flow. *Proc. 3rd Int. Conf. on Laser Anemometry Advances and Applications*, pp. 431–440. Springer, Berlin.

Taylor, G. I. (1940) Generation of ripples by wind blowing over a viscous liquid. Reprinted in *The Scientific Papers of Sir Geoffrey Ingram Taylor*, Vol. 3, pp. 244–255. Cambridge University Press, London.

Teixeira, J. C. F. (1988) Turbulence in annular two phase flow. Ph.D. Thesis, University of Birmingham.

Teixeira, J. C. F., Azzopardi, B. J. and Bott, T. R. (1988) The effect of inserts on drop size in vertical annular flow. *2nd U.K. National Heat Transfer Conf.*, Strathclyde.

Thwaites, G. R., Kulov, N. N. and Nedderman, R. M. (1976) Liquid film properties in two-phase annular flow. *Chem. Engng Sci.* **31,** 481–486.

Tomida, T. and Okazaki, T. (1974) Statistical character of large disturbance waves in upward two-phase flow of air–water mixtures. *J. Chem. Engng Jap.* **7,** 329–333.

Tsuji, Y. and Morikawa, Y. (1982) LDV measurements of an air–solid two phase flow in a horizontal pipe. *J. Fluid Mech.* **120,** 385–409.

Tsuji, Y., Morikawa, Y. and Shiomi, H. (1984) LDV measurements of an air–solid two phase flow in a vertical pipe. *J. Fluid Mech.* **139,** 417–434.

Ueda, T. (1979) Entrainment rate and size of entrained droplets in annular two-phase flow. *Bull. JSME* **22,** 1258–1265.

Ueda, T., Tanaka, H. and Koizumi, Y. (1978) Dryout of liquid film in high quality R-113 upflow in a heated tube. *Proc. 6th Int. Heat Transfer Conf.*, Toronto.

Uijttewaal, W. J. S. and Oliemans, R. V. A. (1996) Particle dispersion and deposirion in direct numerical and large eddy simulations of vertical pipe flows. *Phys. Fluids* **8,** 2590–2604.

Verbeek, P. H. J., Miesen, R. and Schellenkens, C. J. (1992) Liquid entrainment in annular dispersed upflow. *8th Annual Eur. Conf. on Liquid Atomisation and Spray Systems*, Amsterdam, September 30–October 2.

Webb, D. R. and Hewitt, G. F. (1975) Downward co-current annular flow. *Int. J. Multiphase Flow* **2,** 35–49.

Whalley, P. B., Hewitt, G. F. and Hutchinson, P. (1974) Experimental wave and entrainment measurements in vertical annular two-phase flow. *Multi-phase Flow Systems Symp.*, Strathcylde.

Whalley, P. B., Azzopardi, B. J., Pshyk, L. and Hewitt, G. F. (1977) Axial view photograph of waves in annular two-phase flow. UKAEA Report AERE R8787.

Wicks, M. and Dukler, A.E. (1966) In situ measurements of drop size distribution in two-phase flow: a new method for electrically conducting liquids. *Third International Heat Transfer Conf.*, Chicago.

Wilkes, N. S., Azzopardi, B. J. and Thompson, C. P. (1983a) Wave coalescence and entrainment in vertical annular two-phase flow. *Int. J. Multiphase Flow* **9,** 383–398.

Wilkes, N. S., Azzopardi, B. J. and Willetts, I. P. (1983b) Drop motion and deposition in annular two- phase flow. *Proc. Nuclear Reactor Thermal-Hydraulics, ANS*, pp. 202–209.

Willetts, I. P. (1987) Non-aqueous annular two-phase flow. D.Phil. Thesis, University of Oxford.

Wolf, A. (1995) Film structure of vertical annular flow. Ph.D. Thesis, Imperial College, London.

Woodmansee, D. E. and Hanratty, T. J. (1969) Mechanism for the removal of droplets from a liquid surface by a parallel air flow. *Chem. Engng Sci.* **24,** 299–307.

Wurtz, J. (1978) An experimental and theoretical investigation of annular steam water in tubes and annuli at 30 and 90 bar. Riso Report 372.

Zaidi, S.H. and Altunbas, A. (1997) A comparative study of annular two-phase flow using phase Doppler and laser diffraction techniques. *7th Int. Conf. on Liquid Atomization and Spray Systems*, Seoul, Korea, 19–22 August.

Zisselmar, R. and Molerus, O. (1979) Investigation of solid–liquid pipe flow with regard to turbulence modification. *Chem. Engng J.* **18,** 233–239.